

RESEARCH

Open Access



Toxic effects of polystyrene nanoplastics on MDA-MB-231 breast cancer and HFF-2 normal fibroblast cells: viability, cell death, cell cycle and antioxidant enzyme activity

Hanie Sadeghinia¹, Parichehr Hanachi^{1*}, Reihaneh Ramezani² and Samaneh karbalaei¹

Abstract

Background Environmental nanoplastics pose a potential health risk due to human exposure, necessitating studies on their cellular effects. This study aims to assess the toxic and antibacterial properties of polystyrene nanoplastics (PS-NH₂) on MDA-MB-231 breast cancer cells and HFF-2 fibroblast cells, while also evaluating their oxidative stress responses. Additionally, the study explores the anti-tumor effects and apoptosis induction by PS-NH₂. The primary objectives were to determine the cytotoxicity, antibacterial efficacy, and oxidative stress response of PS-NH₂ at different concentrations and sizes. The study also aimed to investigate the mechanism of cell death, including apoptosis, necrosis, cell cycle arrest, and changes in antioxidant enzyme activity (SOD and GPx).

Methods Nanoplastic properties were characterized using FTIR, FESEM, and zeta potential analysis. Antibacterial effects were assessed using the agar dilution method, while the MTT assay determined cytotoxicity in MDA-MB-231 and HFF-2 cells. Apoptosis, necrosis, cell cycle arrest, and antioxidant enzyme activities (SOD, GPx) were also evaluated.

Results FTIR analysis confirmed the amino-functionalization of PS-NH₂ with a wide peak at 3386 cm⁻¹, and zeta potential indicated a neutral charge. PS-NH₂ showed no antibacterial activity against *E. coli* or *Staphylococcus aureus* at sizes of 90, 200, and 300 nm. Cytotoxicity assays revealed dose-dependent decreases in cell viability for both cell lines. SOD and GPx activity decreased significantly with increasing PS-NH₂ concentrations. Both cell lines underwent apoptosis, with cell accumulation in the G1 and sub-G1 phases, indicating apoptotic cell death.

Conclusions PS-NH₂ exhibits dose- and size-dependent cytotoxicity in MDA-MB-231 and HFF-2 cells. Smaller particle sizes and higher concentrations of PS-NH₂ enhance oxidative stress, leading to apoptosis and cell cycle arrest.

Keywords Breast cancer, Nanoplastic, Gpx, Polystyrene, SOD

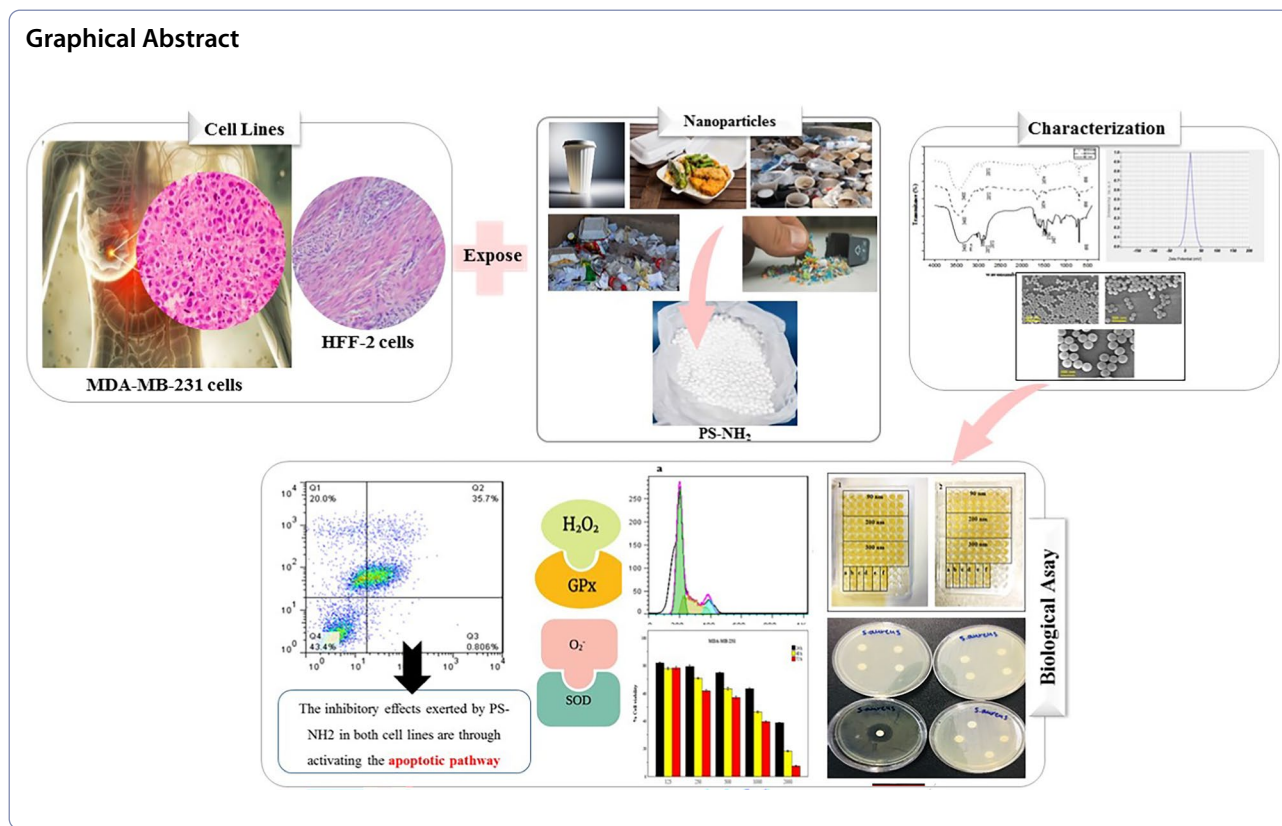
*Correspondence:

Parichehr Hanachi
p.hanachi@alzahra.ac.ir

Full list of author information is available at the end of the article



© The Author(s) 2024. **Open Access** This article is licensed under a Creative Commons Attribution-NonCommercial-NoDerivatives 4.0 International License, which permits any non-commercial use, sharing, distribution and reproduction in any medium or format, as long as you give appropriate credit to the original author(s) and the source, provide a link to the Creative Commons licence, and indicate if you modified the licensed material. You do not have permission under this licence to share adapted material derived from this article or parts of it. The images or other third party material in this article are included in the article's Creative Commons licence, unless indicated otherwise in a credit line to the material. If material is not included in the article's Creative Commons licence and your intended use is not permitted by statutory regulation or exceeds the permitted use, you will need to obtain permission directly from the copyright holder. To view a copy of this licence, visit <http://creativecommons.org/licenses/by-nc-nd/4.0/>.



Introduction

Today, plastic is an inseparable part of the development of civilization. According to recent environmental studies, Plastics, particularly nanoplastics, have become ubiquitous in the environment and are a significant concern due to their persistence and potential toxicity, especially in biological systems [1]. Nanoplastics can be produced from the fragmentation of plastic products in the range of 1-100 nm [2].

According to previous research, nanoplastics have been identified in water, soil, air, and sludge. Polystyrene is one of the most common plastics used in different industries. Polystyrene is made of styrene monomers. Polystyrene is used to produce toys, cup covers, CDs, health and cosmetic industries, etc. Among various types of plastics, polystyrene, made from styrene monomers, is one of the most commonly used in industries such as toy manufacturing, packaging, and cosmetics [3].

Approximately 8 million tons of waste, primarily plastic, are dumped into oceans annually, contributing to 70% of marine pollution. This accumulation of plastic waste has sparked studies on the effects of nanoplastics, particularly polystyrene nanoplastics (PS-NPs), on aquatic species, revealing toxic effects depending on size and exposure levels [4].

More recently, PS-NPs have been detected in the human body. A Dutch study published in Environment International discovered microplastics in human blood, with nearly 80% of participants showing traces of these particles, including PET and polystyrene. These findings suggest the potential for plastics to be transported to human organs through the bloodstream. According to their results, PET plastic (polyethylene terephthalate) streaks were seen in half of the blood samples. This plastic is mainly used in making beverage bottles. This is even though more than a third of them had polystyrene particles. Polystyrene is used to make disposable containers and food packaging for various products. The study added: it is scientifically plausible that plastic particles may be transported to organs through the bloodstream [5–8].

PS-NPs are also prevalent in cosmetic products, particularly scrubs and cleaners. One of the abilities of PS-NH₂ is that it has the ability to dissolve in biological fluids and combine with proteins [9]. Schirinzi et al. [10] conducted a study on two cell lines, brain T98G epithelial HeLa cells, to determine the effect of nanoplastics including PS on ROS and cell viability. These cell lines were exposed to nano and micro-PS particles with 40 to 250 nm diameters, in concentrations of 10 ng/ml to 10 mg/ml. Their research showed that

exposure to PS-NPs caused a significant increase in ROS and a decrease in cell viability in brain epithelial and HeLa cells.

Cancer includes a group of diseases with unregulated cell growth, invasion and metastasis of cells from the original site to other parts of the body [11]. According to WHO estimates, the global incidence of cancer is expected to increase to 30.2 million cases in 2040, almost 50% more than in 2020. In these statistics, female breast cancer has overtaken lung cancer as the most common cancer diagnosed [9].

In another study, human gastric adenocarcinoma (AGS) cells were exposed to 44 and 100 nm unmodified PS-NP and evaluated for cell viability and expression of genes involved in cell cycle regulation. Their results showed that 44 nm PS-NPs were accumulated in the cytosol faster and more effectively. In addition, they stated that PS-NP affected the viability and morphology of AGS cells and the presence of polystyrene nanoparticles led to the induction of inflammation. Also, exposure to PS-NP for AGS cells had a significant effect on the expression of genes related to cell cycle regulation [12].

In another study, different cell lines, including 1321N1, HepG2, HEK 293, were incubated with nanoparticles with a diameter of 50 nm and concentrations from 0.3 to 100 mg/ml for 24 and 72 h. They showed that amine-modified polystyrene nanoparticles had a cytotoxic effect, which caused damage to the cell membrane. In addition, nanoparticles cause apoptosis, which activates caspase 9 and two executive caspases 3 and 7 [11].

Ishita Pan et al. (2023) focus on how biofilms grow on the surfaces of microplastics, the factors affecting the growth of these biofilms and the effects caused by the accumulation of metals in these biofilms, which can cause neurotoxicological consequences (toxic to the nervous system) in the human body. The article also mentions strategies to restore the homeostasis of metals in the body. Therefore, it introduces a new approach about the risks of heavy metals associated with microplastic biofilms, which microplastics act as carriers of heavy metals and cause metal imbalances in the human body [13].

Karthikeyan Kandaswamy et al. (2024) investigated the possible ecotoxicological effect of single and combined simultaneous exposure to polystyrene nanoparticles (PS-NPs) and diclofenac (DCF) in zebrafish (*Danio rerio*). They found that exposure affected all biomarkers assessed in the zebrafish larval toxicity analysis. According to their study, simultaneous exposure to PS-NPs and DCF showed an adverse effect on the gut region, supporting the idea that PS-NPs synergistically aggravated the toxicity of DCF in zebrafish [14].

Seenivasan Boopathi et al. (2023) investigated the combined effects of a high-fat diet (HFD) and polyethylene microplastics (PE-MP) in a zebrafish (*Danio rerio*) model, aiming to uncover the underlying molecular mechanisms. Histological and gene expression analyses showed significant liver inflammation and damage in zebrafish exposed to both HFD and PE-MP, resembling the characteristics of non-alcoholic fatty liver disease (NAFLD). The researchers found that lipid accumulation in the fish tissues increased when HFD was combined with PE-MP exposure, indicating that microplastics may disrupt normal fat metabolism, raising the risk of excessive fat deposition. Additionally, PE-MP exposure triggered oxidative stress in the zebrafish [15].

Ajay Guru et al. [16] discuss polyethylene microplastics (PE-MP), small plastic particles that are widespread and long-lasting environmental pollutants, and ABM pesticides, commonly used chemicals that may harm non-target organisms. The study's findings suggest that the combined exposure to microplastics and pesticides can lead to complex, context-dependent interactions, with potentially synergistic effects resulting in greater toxicity than exposure to either pollutant alone. The mechanisms responsible for these combined effects are explored in the research.

According to the serious censuses reported by the World Health Organization, it is necessary and important to investigate the effective factors in the incidence of breast cancer.

The use of MDA-MB-231 cells in nanoplastic research is conducted for the following reasons: this cell line is a highly aggressive, triple-negative breast cancer (TNBC) model characterized by poor differentiation and the absence of estrogen receptor (ER), progesterone receptor (PR), and HER2 (human epidermal growth factor receptor 2) expression. In summary, MDA-MB-231 cells are utilized in nanoplastic research due to their unique properties in studying invasive cancer and evaluating the potential impact of environmental agents, such as nanoplastics, on cancer progression and cell death. HFF-2 cells, due to their natural and fibroblastic nature, serve as an important tool for studying the effects of nanoplastics on healthy cells and assessing their toxicity in comparison to cancer cells. The aim of this study is to evaluate the toxic effects of PS-NPs with different functional groups on MDA-MB-231 breast cancer cells and HFF-2 fibroblast cells, focusing on uptake, cell viability and biological response. The results provide valuable insights into the distribution and potential health risks of PS-NPs in human cells and provide a better understanding of their role in oxidative stress and cytotoxicity.

Materials and methods

Preparation of materials

MDA-MB-231 and HFF-2 cells were obtained from the Stem Cell Technology Research Center (Tehran, Iran). These particles were selected due to their widespread use in environmental toxicity studies. The experiments performed and the results obtained can have a significant impact on protocols for the use of products containing these particles worldwide.

PS-NH₂ nanoparticles with sizes of 90, 200, and 300 nm were acquired from Tianjin Saierqun Technology (China) as a 2.5% aqueous suspension and were stored at 4 °C.

Characterization of PS-NPs

Before use, PS-NH₂ nanoparticles were prepared according to the method described by Fadare et al. [17] for all experiments. The stock solutions of PS-NH₂ and the required concentrations were prepared by diluting the stock with deionized water [18]. Particle size distribution and morphology were analyzed using a FE-SEM ZEISS Sigma 300 scanning electron microscope. Additionally, the compounds and bonds in organic and inorganic materials were identified, and the amine content of the particles was confirmed using Fourier-transform infrared (FTIR TENSOR 27) spectroscopy and X-ray diffraction (XRD Xpert Pro Panalytical), both of which are subsets of spectroscopic analysis.

Cell culture

MDA-MB-231 and HFF-2 cells were cultured in Dulbecco's Modified Eagle Medium (DMEM, USA, Gibco) High Glucose culture medium, supplemented with 10% fetal bovine serum (FBS, Gibco, USA) and 1% penicillin–streptomycin antibiotic solution (PenStrep, Gibco, USA). These cells were incubated at 37 °C with humidity and 5% CO₂ for optimal growth. Through documentation, monitoring, and continuous or periodic logging of temperature, CO₂, and humidity data from the incubator, it can be confirmed that these conditions remained stable throughout the entire incubation period. After reaching sufficient growth, the cells were enzymatically detached from the cell culture flask using trypsin-EDTA (25%, Gibco, USA). Cell counts were performed with a Neubauer slide (hemocytometer) to assess the necessary tests. The culture medium inside the flask was changed every 2 days if cells were growing on the bottom of the flask. When the cells reached approximately 80% confluency at the bottom of the flask, they were passaged to

support further growth and prevent cell death. All samples in this study were repeated three times.

Cell viability assay

The cytotoxicity of polystyrene nanoplastics was evaluated by assessing the growth and proliferation of cancer cells and fibroblasts. The IC₅₀ of these compounds was determined using the MTT colorimetric method. [19]. The cytotoxicity of PS-NPs was evaluated using (4,5-dimethylthiazol-2-yl)-2,5-diphenyltetrazolium bromide. MDA-MB-231 and HFF-2 cells were cultured in 96-well plates for 24, 48, and 72 hours and treated with PS-NPs at concentrations of 125, 250, 500, 1000, and 2000 mg/ml. MDA-MB-231 and HFF-2 cells without PS-NPs were used as controls, while wells without cell inoculation served as blanks.

After the incubation period, MTT solution was added to all wells and incubated for 2–4 h at 37 °C with 5% CO₂ to allow the purple precipitate at the bottom of the plate to become visible. The precipitate was then dissolved in 100 µl of DMSO, and the absorbance of the formazan solution was measured at 570 nm using an ELISA reader (Citation™ Biotek, USA).

All stages after incubation with PS-NPs were observed under an inverted microscope. The survival percentage was calculated by subtracting the blank absorbance from the sample absorbance at 570 nm using the following formula:

$$\text{Cell viability(\%)} = \frac{\text{Abs(570)treatment} - \text{Abs(570)blank}}{\text{Abs(570)control} - \text{Abs(570)blank}} \times 100.$$

Disc diffusion method

The antimicrobial activity of PS-NPs against pathogenic strains of *Escherichia coli* and *Staphylococcus aureus* was studied using the disk diffusion method. For this method, 100 microliters of the microorganism were evenly spread on a plate containing Mueller-Hinton agar (MHA) and incubated at 37 °C. Thirty microliters of nanoparticles at different concentrations (250, 500, 1000, and 2000 mg/ml) were poured onto the disks using blank disks, and the disks were left for a few minutes to allow for complete absorption of the nanoparticles.

After the incubation period, the growth halo around each disk was measured and compared. The diameters of the inhibition zones were recorded using a ruler. All experiments were performed in triplicate, and the average standard errors were calculated.

Minimum inhibitory concentration (MIC)

In this method, serial dilutions of nanoparticles with sizes of 90, 200, and 300 nm were prepared in the wells of a 96-well plate, and then 1/100 of 0.5 McFarland's (10⁸ ×

1.5 CFU/ml) was added to each well. For each nanoparticle, a positive control (nanoparticle + Mueller-Hinton broth culture medium) and a negative control (Mueller-Hinton broth culture medium + 0.5 McFarland's) were included. The plate was incubated for 24 h at 37°C, and the absorbance was measured at a wavelength of 600 nm using an ELISA reader. All particles and concentrations were repeated three times.

Apoptosis and necrosis

To determine the type of induced cell death (apoptosis and necrosis) in breast adenocarcinoma cells, the flow cytometric technique was performed using Annexin V-FLUOS and PI staining according to the instructions of the eBioscience kit (Thermo Fisher). The device used for this test was the BD FACSCalibur™ II flow cytometer (USA).

Based on the results of cytotoxicity, two concentrations of each polystyrene nanoparticle 2000 and 500 (IC₅₀) were used to evaluate apoptosis and necrosis. The cells were cultured in a 24-well plate, and after treatment with the specified concentrations for 48 h, the cells were detached from the bottom of the wells using trypsin and centrifuged for 3 min at 1700 rpm. Finally, the pellet was resuspended in FBS serum and stained with Annexin V-FLUOS and PI dyes.

Cell cycle

To perform the cell cycle analysis, the cells were washed with PBS buffer. After trypsinization, the cells were centrifuged at 1700 rpm for 5 minutes. Then, the cells were cultured in a 24-well plate based on cell counting. After 24 hours, the cells were treated with nanoparticles at the IC₅₀ concentration of 2000 mg/ml. Following treatment, the cells were incubated for 48 hours in an incubator at 37 °C with 5% CO₂. The control in this experiment consisted of cells without treatment. After the incubation period, the cells were centrifuged (1700 rpm) for 3 min, and the resulting pellet was resuspended in FBS serum for analysis using flow cytometry.

Oxidative response assay

MDA-MB-231 and HFF-2 cells were seeded in a 6-well plate at a density of 10⁶ cells/well. After 24 h, these cells were co-incubated with concentrations of 500 and 1000 mg/ml of PS-NPs. In addition, MDA-MB-231 and HFF-2 cells were incubated as controls without exposure to PS-NPs. After 48 hours, the medium was removed from the plate, and the cells were washed three times with PBS. Five hundred microliters of lysis buffer was added to the wells for 30 minutes. The samples were then centrifuged at 12,000 rpm for 5 min at 4 °C, and the supernatant was used as a sample.

The activity of cellular superoxide dismutase (SOD) and glutathione peroxidase (GPX) was evaluated using diagnostic kits (KIAZIST, Iran) according to the manufacturer's instructions. Subsequently, the total protein concentration of the cells in each well was measured using a BCA kit. The detected values of SOD and GSH content were normalized to the total protein content of the samples.

Statistical analysis

All assays in this study were performed in triplicate. The obtained results are expressed as mean ± standard deviation (SD). For statistical analysis of the data, two-way analysis of variance (ANOVA) with post hoc Bonferroni and Tukey tests was used to compare significant differences between biological parameters for the control and treatment groups. *P*-values < 0.05 and < 0.001 were considered statistically significant.

Results

Characteristics of PS-NPs

The results of the IR spectrum related to polystyrene nanoplastics are shown (Fig. 1a). According to the results obtained from FTIR analysis, it can be seen that the broad absorption peak at 3386 cm⁻¹ is related to the stretching bond of the first type of amine N–H and the bending peak at 1580–1650 cm⁻¹ is related to the amine vibration of N–H. The appearance of medium and sharp peaks in the region of 2082–3026 cm⁻¹ is characteristic of C–H aromatic stretching vibrations.

The absorption band observed at 730–765 cm⁻¹ indicates the presence of a strong C=C bending and alkene bond. The broad and strong peak at 3400 cm⁻¹ indicates the existence of O–H bond [20]. According to the FESEM microscope images, PS-NPs have been synthesized in a spherical shape with a uniform and regular appearance. These images were taken with a magnification of 500 nm (Fig. 1b). The higher the value (positive or negative), the more stable the colloidal dispersion. After examining the zeta potential, PS-NH₂ nanoparticles were found to have an electrical charge of 17.3–15.9 mV, where the zeta potential is close to zero (that is, the sample is approximately at the isoelectric point) and has a neutral electrical charge. Therefore, according to the obtained results, PS-NH₂ nanoparticles, due to their surface charge range, cause the instability of the particles and this provides the possibility for flocculation and non-separation of the particles (Fig. 1c) [21].

Effect of PS-NPs on MDA-MB231, HFF-2 cell viability

HFF-2 cells are spindle-shaped and elongated, while MDA-MB-231 cells appear polygonal. Figure 2-3 illustrates the morphology of HFF-2 and MDA-MB-231

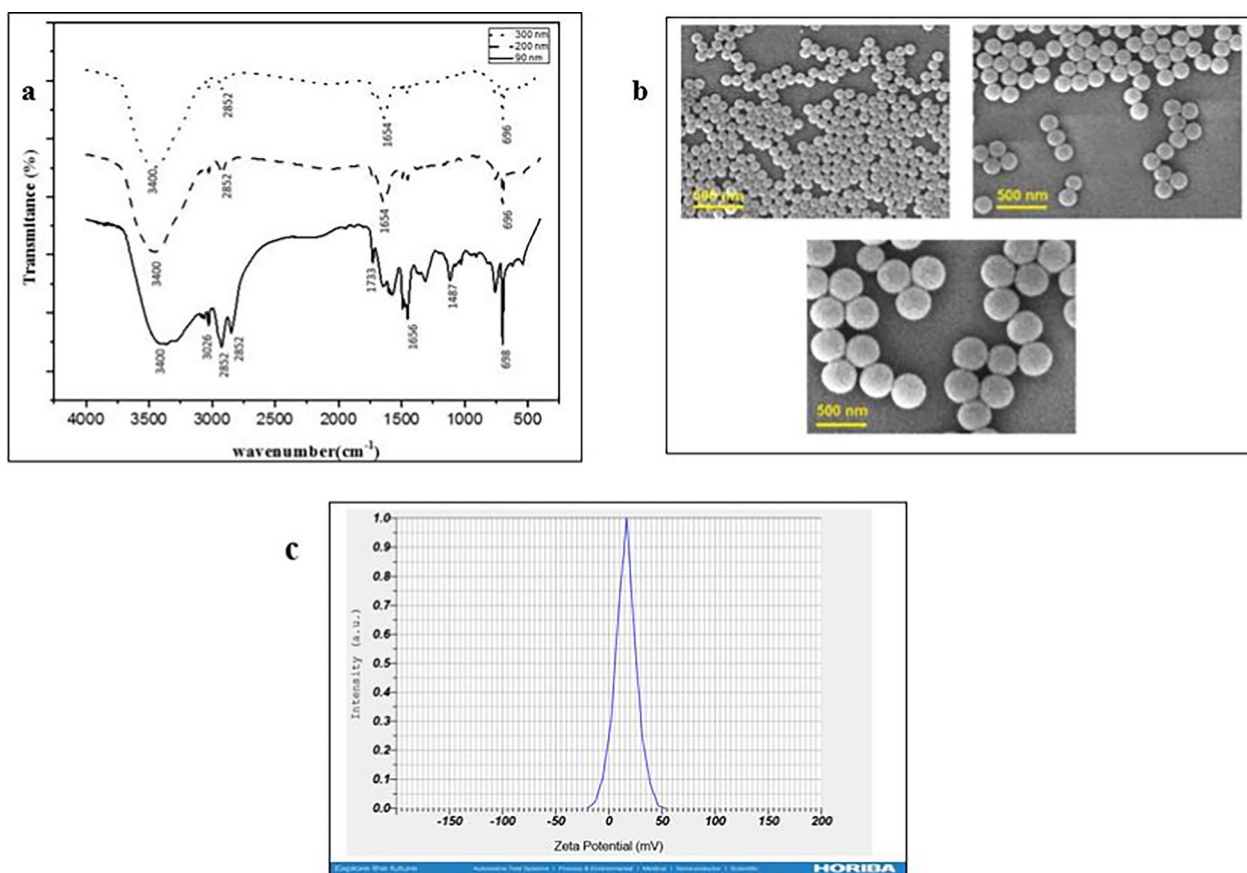


Fig. 1 **a** FTIR spectroscopy. **b** PS-NH₂ nanoparticles are shown by FESEM scanning electron microscope to be spherical with regular and uniform appearance. These images were taken with a magnification of 500 nm. **c** The zeta potential of PS-NH₂ nanoparticles indicates that the electric charge of these particles is approximately neutral

cells. The effect of different concentrations of PS-NH₂ on MDA-MB-231 and HFF-2 cell lines was investigated through cell culture (Figs. 4, 5). According to the results obtained in this study, in both MDA-MB-231 and HFF-2 cell lines, it was observed that the toxicity effect of PS-NH₂ nanoparticles increased with rising concentration and over time. Furthermore, smaller nanoparticle sizes exhibited a greater toxicity effect [20].

The goal of this study is to investigate the anti-tumor effects and apoptosis-inducing properties of a nanoplastic polystyrene combination. In the MTT assay, the color intensity produced is proportional to the number of cells with active mitochondria. In other words, this method is used to determine the rate of cell proliferation and survival after exposure to cytotoxic substances [20]. The results of the two-way analysis of variance (ANOVA) show that the effects of time, concentration, and size of PS-NH₂ nanoparticles on the survival of breast cancer cells are significant ($p < 0.001$) (Table 1) [20].

An independent *t*-test was used to compare the viability of MDA-MB-231 cells with HFF-2 cells. As the

results of the independent *t*-test show, the average survival of MDA-MB-231 cells is not significantly different from that of HFF-2 cells. Therefore, it can be concluded that the viability of both cell types is generally the same (Figs. 4, 5).

Antibacterial effect PS: agar dilution

Polystyrene nanoparticles in three sizes of 90 nm, 200 nm, and 300 nm were investigated to determine their antimicrobial properties against Gram-positive *S. aureus* and Gram-negative bacteria. The antibiotic streptomycin was used as a positive control to assess the sensitivity of the species (Fig. 6g), while the culture medium with nanoparticles served as a negative control (Fig. 6h). A comparison of the results for the nanoparticles with the controls indicated that these particles, at concentrations of 500, 1000, 1500, and 2000 µg/ml, had no antimicrobial effect on either of the two bacteria, and no growth halo was observed (Fig. 6). In addition, the MIC results confirm that the combination of PS-NH₂ did not inhibit

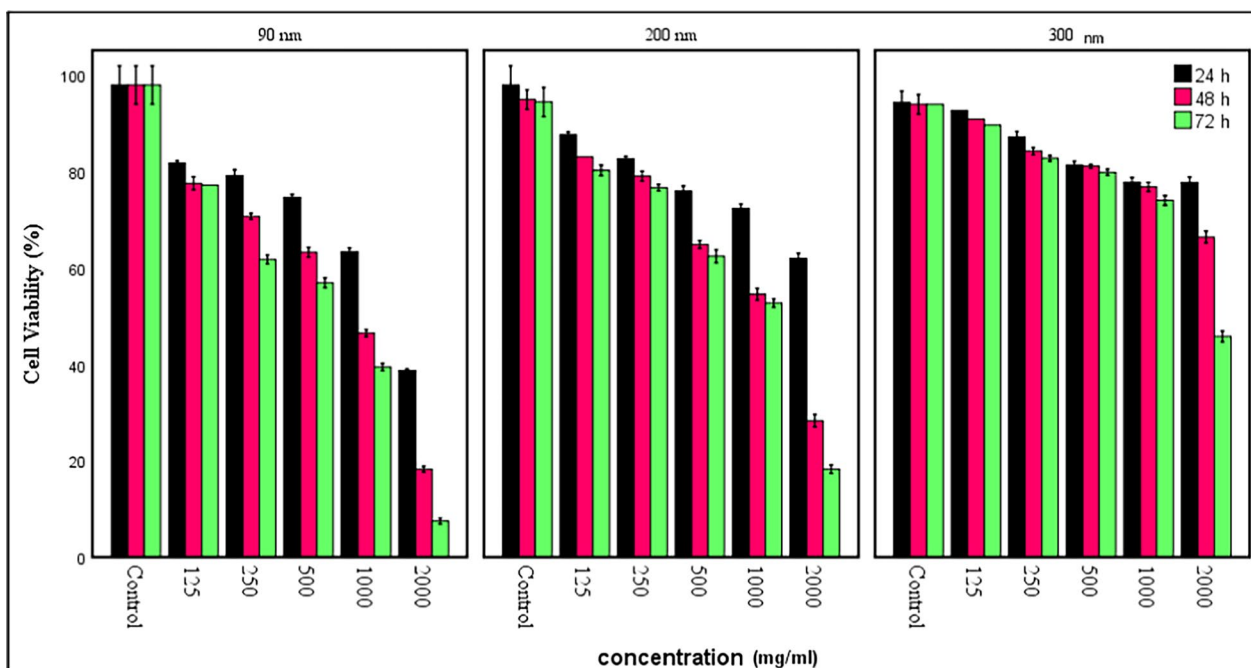


Fig. 2 The MDA-MB-231 cells morphological changes caused by PS-NH₂ (a), MDA-MB231 control cells (b) exposure at dosages of 125 µg/mL (c), 250 µg/mL (d), 500 µg/mL (e), 1000 µg/mL (f), 2000 µg/mL in 90 nm

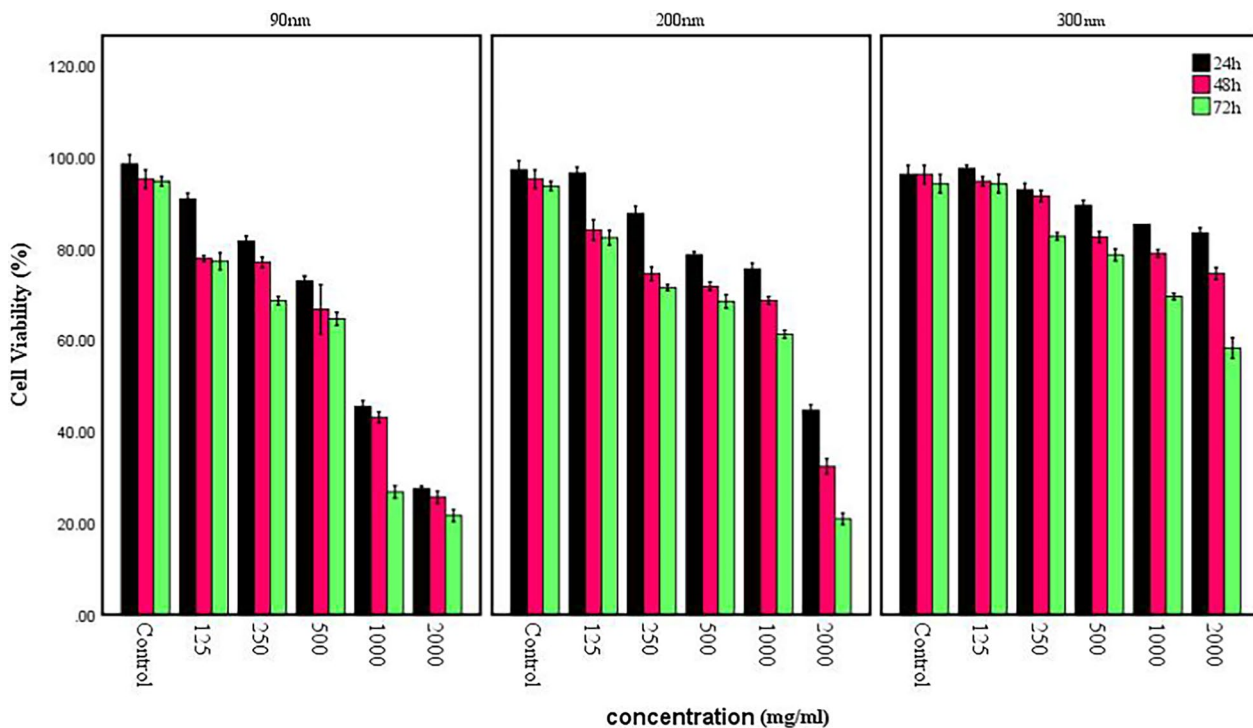


Fig. 3 The HFF-2 cells morphological changes caused by PS-NH₂ (a), HFF-2 control cells (b) exposure at dosages of 125 µg/mL (c), 250 µg/mL (d), 500 µg/mL (e), 1000 µg/mL (f), 2000 µg/mL in 90 nm

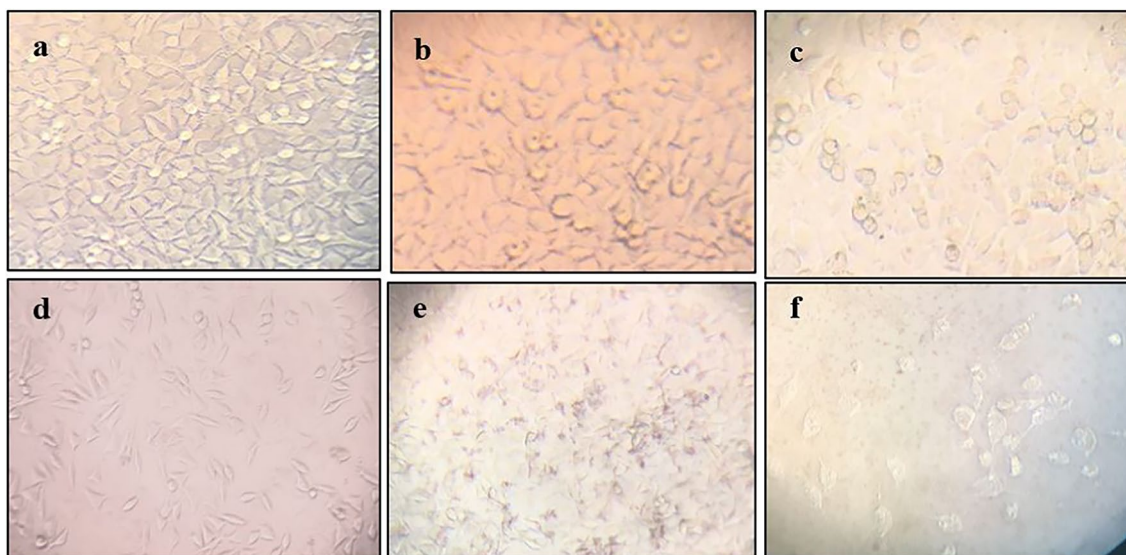


Fig. 4 MDA-MB-231 cell viability exposed to PS-NH₂ sizes 90, 200, 300 nm in 24, 48 and 72 h. ($P < 0.001$)

bacterial growth in any of the wells. Therefore, PS-NH₂ has no antimicrobial effect on *S. aureus* and *E. coli*.

Antibacterial effect of PS: minimum inhibitory concentration (MIC)

Polystyrene nanoparticles in sizes of 90 nm, 200 nm, and 300 nm were investigated to determine their antimicrobial properties against the Gram-positive bacteria *S. aureus* and the Gram-negative bacteria *E. coli*. Mueller-Hinton broth culture medium with 0.5 McFarland bacteria was used as a negative control (Fig. 7b), while streptomycin antibiotic served as a positive control (Fig. 7a). After analysis using an ELISA reader, no antibacterial effect was observed following treatment with PS-NH₂. Similarly, in the antimicrobial test using dilution agar, no growth halo was observed due to the use of PS-NH₂. The results of the MIC and dilution agar tests also confirmed that PS-NH₂ nanoparticles do not exhibit antibacterial effects against *S. aureus* and *E. coli* (Fig. 7 [27]).

Apoptosis

To determine the apoptotic or necrotic effects of PS-NH₂ on MDA-MB-231 and HFF-2 cell lines, we employed flow cytometry and compared the results with the control. In both MDA-MB-231 and HFF-2 cells, it was observed that as the concentration of PS-NH₂ nanoparticles increased, the percentage of living cells decreased, leading them to

enter the phases of apoptosis and necrosis. Additionally, as the nanoparticle size increased, its effect decreased in both cell types. Statistically, the samples treated with PS-NH₂ nanoparticles in both MDA-MB-231 and HFF-2 cell lines showed a significant difference compared to the control sample (Figs. 8, 9a–g) ($P < 0.001$).

In this research, flow cytometry analysis was utilized for further studies on the method of cell death (apoptosis or necrosis). Our results indicated that the percentage of apoptotic cells (annexin positive and PI negative) increased with the passage of time, higher concentrations, and smaller sizes of PS-NH₂. According to the obtained results, increasing the concentration from 500 µg/ml to 2000 µg/ml and reducing the size of PS-NH₂ to 90 nm significantly increased the percentage of apoptosis ($P < 0.001$).

The highest percentage of apoptosis induced was 50% in HFF-2 cells at a concentration of 500 µg/ml of 90 nm PS-NH₂ after 48 h of treatment (Fig. 9a).

Cell cycle

In the cell cycle, a regular and organized sequence of events occurs until replication takes place, which can be divided into two general stages: interphase and mitosis [28]. According to the obtained results, MDA-MB-231 and HFF-2 cells are predominantly arrested in the G1 and sub-G1 phases (Fig. 10). This finding indicates the occurrence of apoptosis as a result of treatment with

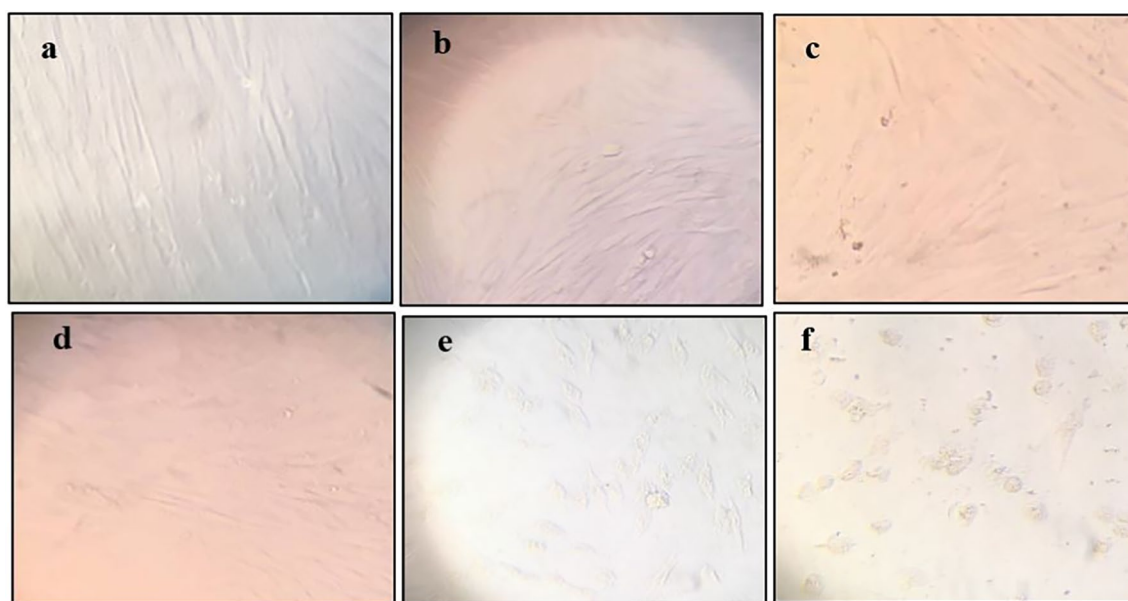


Fig. 5 HFF-2 cell viability exposed to PS-NH₂ sizes 90, 200, 300 nm in 24, 48 and 72 h. ($P < 0.001$)

Table 1 Description of relevant studies reporting the cytotoxic effects of PS-NPs in human cell lines

Human cell lines	NPs type	NPs size (nm)	NPs dosage ($\mu\text{g/mL}$)	Exposure time	Cytotoxicity		Reference
					Cell viability	Other effects	
MDA-MB-231	PS-NH ₂	90, 200, 300	125, 250, 500, 1000, 2000	24, 48, 72	This study	Oxidative damage Prolonged G0/G1 phase in cell cycle	This study
HFF-2	PS-NH ₂	90, 200, 300	125, 250, 500, 1000, 2000	24, 48, 72	This study	Oxidative damage Prolonged G0/G1 phase in cell cycle	This study
HepG2	PS-COOH PS-NH ₂	50	10, 50, 100	24	PS-COOH: 91%, 65%, 54% (10, 50, 100 $\mu\text{g/mL}$) PS-NH ₂ : 92%, 73%, 53% (10, 50, 100 $\mu\text{g/mL}$)	Oxidative damage	[20]
FuB-1	PS	100	10	24	40%	Oxidative damage	[22]
Caco-2	PS	50	200	24, 48	78% (24 h) 72% (48 h)	Genotoxicity DNA oxidative damage	[23]
A549	PS	25, 70	30 (25 nm) 300 (70 nm)	24	50% (25 nm) 85% (70 nm)	Launched inflammatory responses and apoptosis	[18]
AGS	PS	44, 100	10	24	85% (44 nm) 120% (100 nm)	Morphological change	[12]
HeLa	PS-COOH PS-NH ₂	50	50	24	PS-COOH: 98% PS-NH ₂ : 60%	Prolonged G0/G1 phase in cell cycle	[24]
HepG2	PS	15	1.0	24	Did not produce significant cytotoxicity	Gene expression altered	[25]
BEAS-2B	PS-NH ₂	60		16	25%	Not reported	[26]

PS-NH₂ nanoparticles. It was observed that the percentage of apoptosis induced in HFF-2 cells after treatment was higher than that in breast cancer cells. Statistically, both investigated cell lines exhibited a significant difference compared to the control sample ($p < 0.001$).

Examining the results of the cell cycle in the samples treated with PS-NH₂ in the present study demonstrates the role of this compound in creating a disruption in the G1 phase of the cell cycle in MDA-MB-231 and HFF-2 cells. The induction of cell accumulation in the G1 phase by PS-NH₂ is evidenced by the increase in the concentration of this compound (Fig. 10).

The increase in the number of cells in the G1 phase due to treatment with PS-NH₂ at sizes of 200 nm, 90 nm, and 300 nm, in concentrations of 500 and 2000 µg/ml, was significant compared to the control. ($p < 0.001$). The effect of different concentrations of PS-NH₂ is to cause an interruption in the G1 phase of the cell cycle, leading to an increased accumulation of MDA-MB-231 and HFF-2 cells in this phase, which is elevated compared to the control ($P < 0.001$) (Fig. 10, 11).

In HFF-2 cells, the percentage of cells in the G1 phase is lower than that in MDA-MB-231 cells at the same concentration (Fig. 12). Although this treatment significantly affected the number of cells in the G1 and sub-G1 phases in HFF-2 cells compared to the control, it caused an interruption in the G1 phase, leading to the induction of apoptosis in these cells ($p < 0.001$). The percentage of cells in the G1 phase at a size of 90 nm is lower than that at 200 nm, and in these sizes, we observe a decrease in the number of cells in the G1 phase with increasing concentration. At a concentration of 2000 µg/ml of 300 nm PS-NH₂, the percentage of G1 cells is higher than that at 500 µg/ml (Fig. 12a–g). In MDA-MB-231 cells, at sizes of 90 nm and 200 nm, the number of S-phase cells decreases with decreasing concentration. However, at 300 nm, there is an increase in the number of S-phase cells as concentration decreases (Fig. 11a–g). In HFF-2 cells, the percentage of S-phase cells increases as the concentration of PS-NH₂ decreases. Additionally, with an increase in the size of PS-NH₂, the percentage of S-phase cells also rises. The percentage of cells in the G2 phase in the cell cycle of MDA-MB-231 increases from 2000

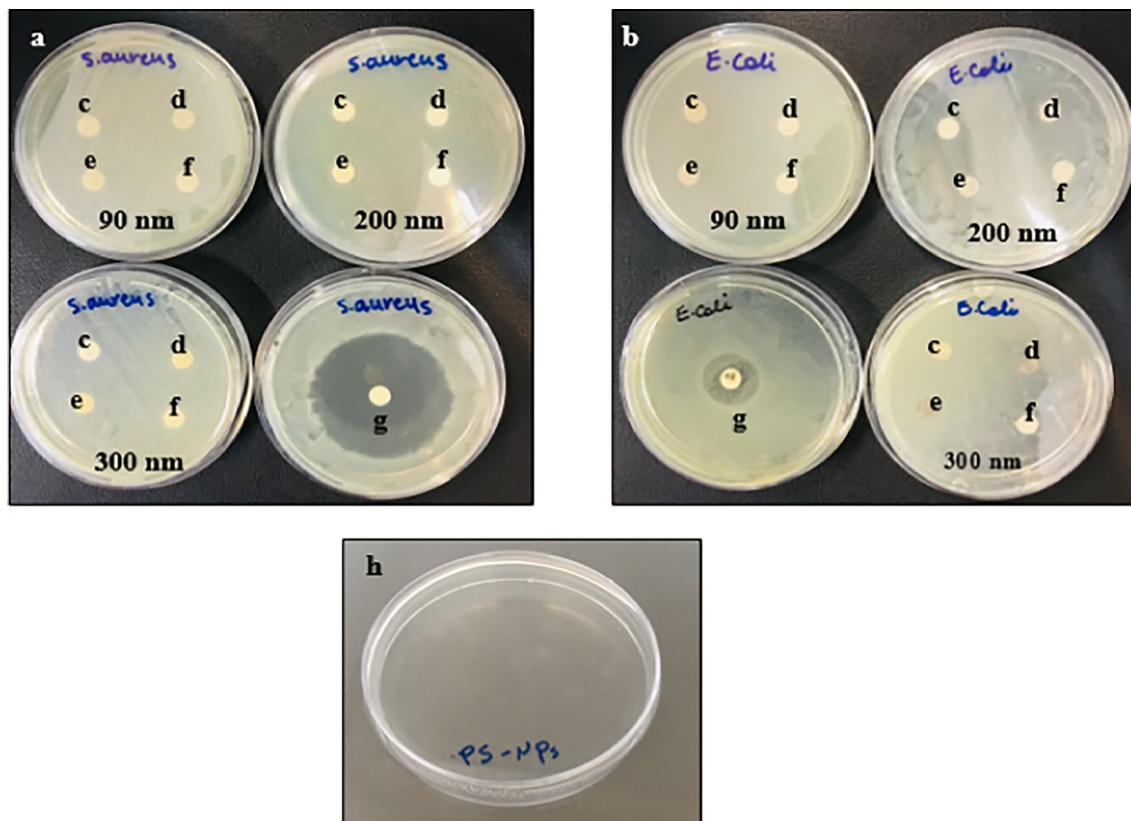


Fig. 6 No formation of growth halo. **a** Staphylococcus aureus bacterium **b** E. coli bacterium exposed to polystyrene nanoplastic in **c-d** concentrations of 500, 1000, 1500, 2000 µg/ml, respectively, in three nanoparticle sizes 90, 200, 300 nm, **g** antibiotic streptomycin, gentamicin as positive control, **h** combination of nanoparticles with Mueller–Hinton broth culture medium as a negative control

to 500 µg/ml, whereas this amount decreases in HFF-2 cells. As the size of PS-NH₂ increases in HFF-2 cells, the amount of G2 cells increases. Overall, the level of G2 is higher in HFF-2 cells compared to MDA-MB-231 cells (Fig. 10).

Activity of antioxidant enzymes

GPx enzyme activity was measured in MDA-MB-231 cells compared to the control (Fig. 13). According to the obtained results, after the cells were exposed to PS-NH₂ nanoparticles with a size of 90 nm at a concentration of 500 µg/ml, the enzyme activity increased approximately 2.3 times compared to the control. At a concentration of 1000 µg/ml, the enzyme activity decreased by 6.5 times compared to the control. Among the tested groups, a decrease in the concentration of PS-NH₂ resulted in a 13-fold increase in enzyme activity, and this difference was statistically significant ($P < 0.001$).

GPx enzyme activity was measured in MDA-MB-231 cells compared to the control. According to the obtained results, after the cells were exposed to PS-NH₂ nanoparticles with a size of 200 nm at a concentration of 500 µg/ml, the enzyme activity was approximately 1.5 times that of the control. At a concentration of 1000 µg/ml, the enzyme activity was halved compared to the control. Among the tested groups, a decrease in the concentration of PS-NH₂ resulted in a 2.5-fold increase in enzyme activity, and this difference was statistically significant ($P < 0.001$).

GPx enzyme activity was measured in MDA-MB-231 cells compared to the control. According to the obtained results, after the cells were exposed to PS-NH₂ nanoparticles with a size of 300 nm at a concentration of 500 µg/ml, the enzyme activity decreased to 0.24 times that of the control. At a concentration of 1000 µg/ml, the enzyme activity was halved compared to the control. Among the tested groups, a decrease in PS-NH₂ concentration resulted in a 1.5-fold increase in enzyme activity, and this difference was statistically significant ($P < 0.001$). Thus, according to the results of the present study, a lower concentration of this nanoparticle is associated with higher activity of the GPx enzyme. GPx enzyme activity was measured in HFF-2 cells compared to the control (Fig. 13). According to the obtained results, after the cells were exposed to PS-NH₂ nanoparticles with a size of 90 nm at a concentration of 500 µg/ml, the enzyme activity was approximately 1.3 times that of the control. At a concentration of 1000 µg/ml, the enzyme activity doubled compared to the control. Among the tested groups, as the concentration of PS-NH₂ increased, enzyme activity decreased to about 0.68 times that of the control, and this difference was statistically significant ($P < 0.001$).

GPx enzyme activity was measured in HFF-2 cells compared to the control. According to the obtained results, after the cells were exposed to PS-NH₂

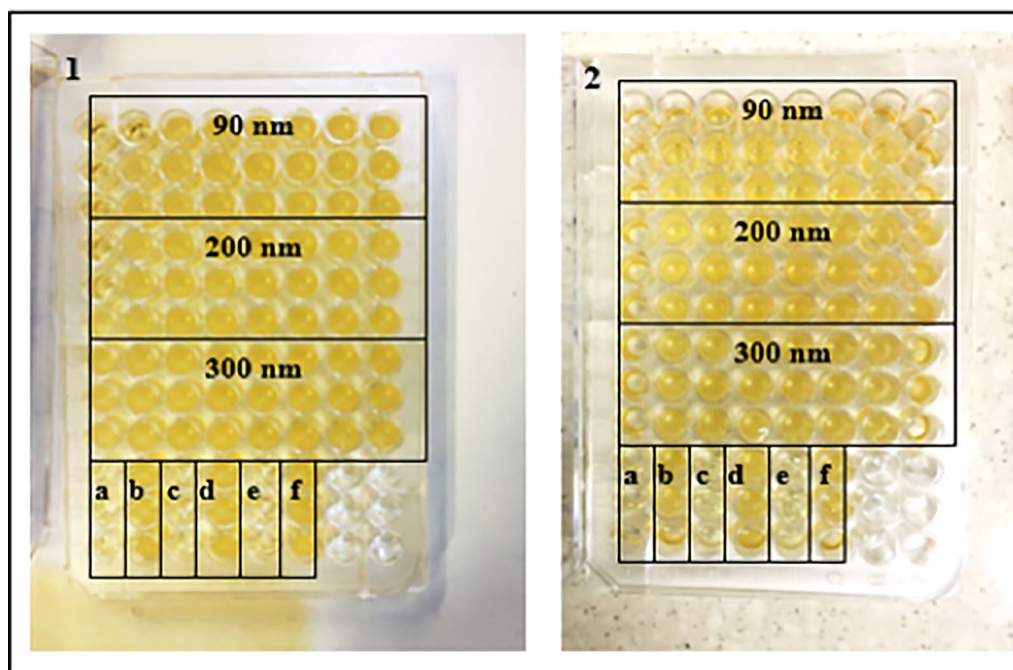


Fig. 7 The effect of PS-NH₂ to determine the lowest inhibitory concentration of 1) *E. coli* 2) *S. aureus*. **a** Positive control 90 nm, **b** negative control 90 nm, **c** positive control 200 nm, **d** negative control 200 nm, **e** positive control 300 nm, **f** negative control 300 nm

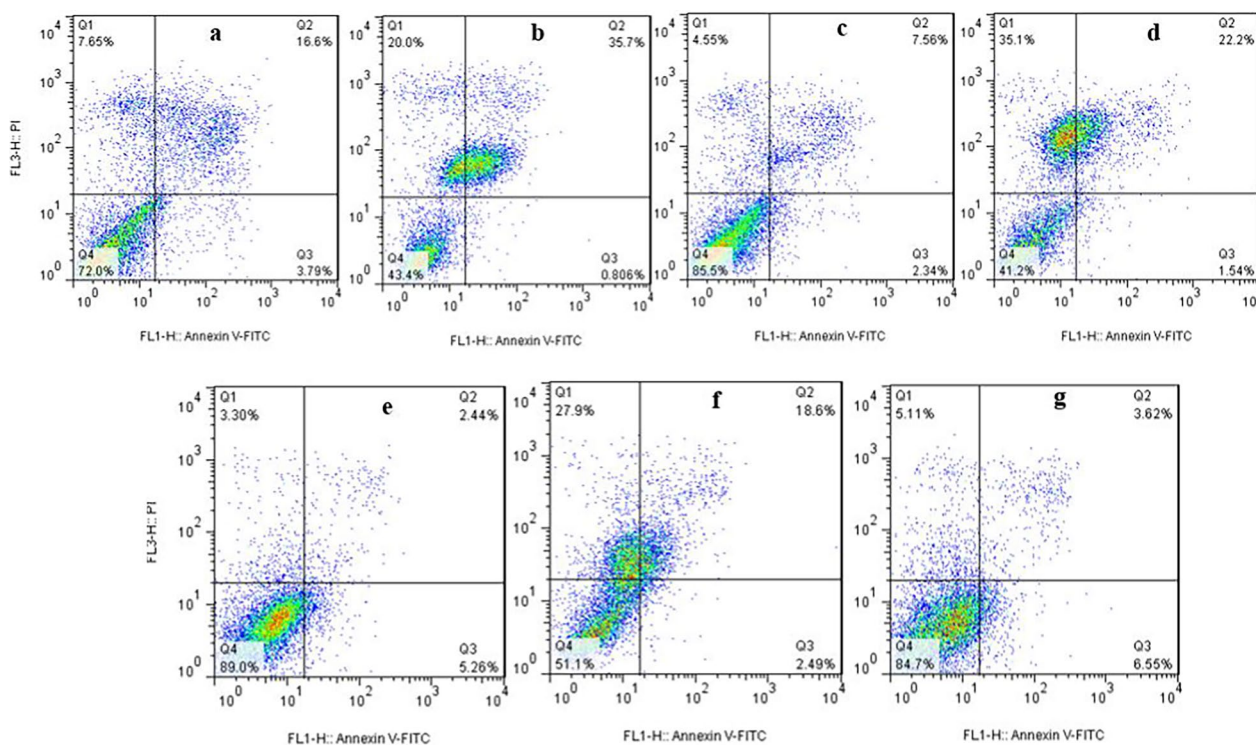


Fig. 8 Flow cytometry results of MDA-MB 231 cells exposed to PS-NH₂ nanoparticles after 48 h. **a** Concentration of 500 µg/ml, size 90 nm. **b** Concentration of 2000 µg/ml size 90 nm. **c** 500 µg/ml size 200 nm. **d** 2000 µg/ml size 200 nm. **e** 500 mg µg/ml size 300 nm. **f** 2000 µg/ml size 300 nm. **g** MDA-MB 231 cell as a control without the presence of PS-NH₂ nanoparticles after 48 h

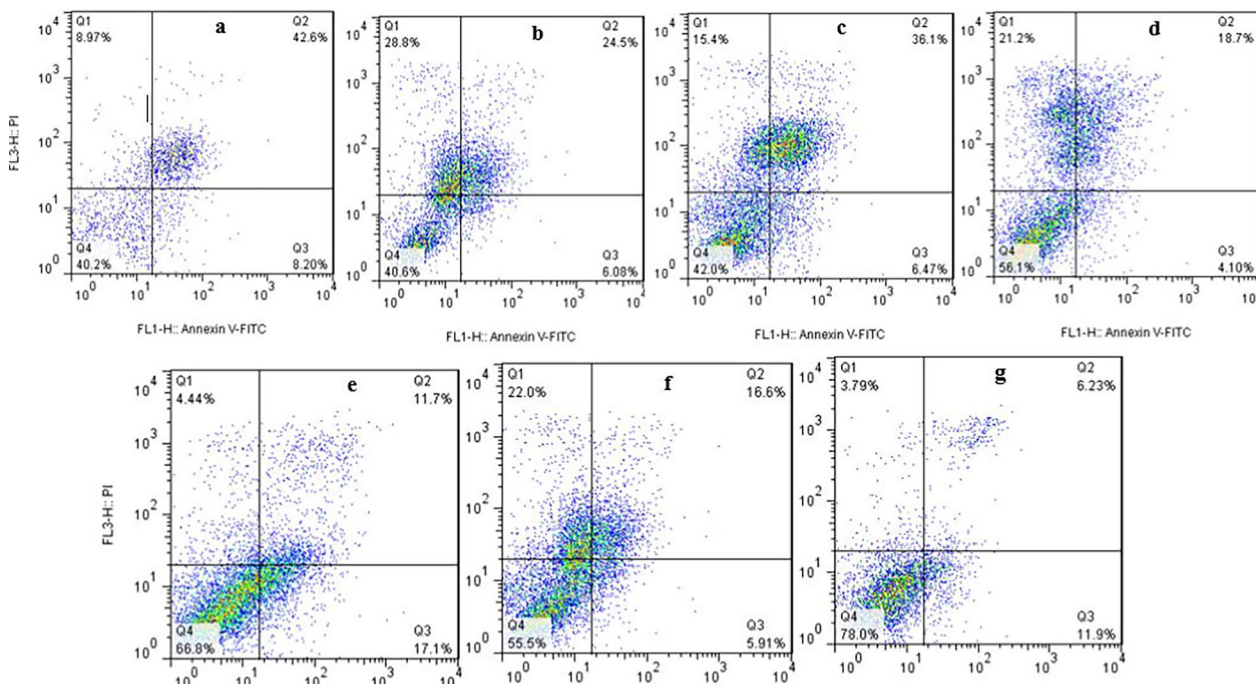


Fig. 9 Flow cytometry results of HFF-2 cells exposed to PS-NH₂ nanoparticles after 48 h. **a** concentration of 500 µg/ml, size 90 nm. **b** Concentration of 2000 µg/ml size 90 nm. **c** 500 µg/ml size 200 nm. **d** 2000 µg/ml size 200 nm. **e** 500 mg µg/ml size 300 nm. **f** 2000 µg/ml size 300 nm. **g** MDA-MB 231 cell as a control without the presence of PS-NH₂ nanoparticles after 48 h

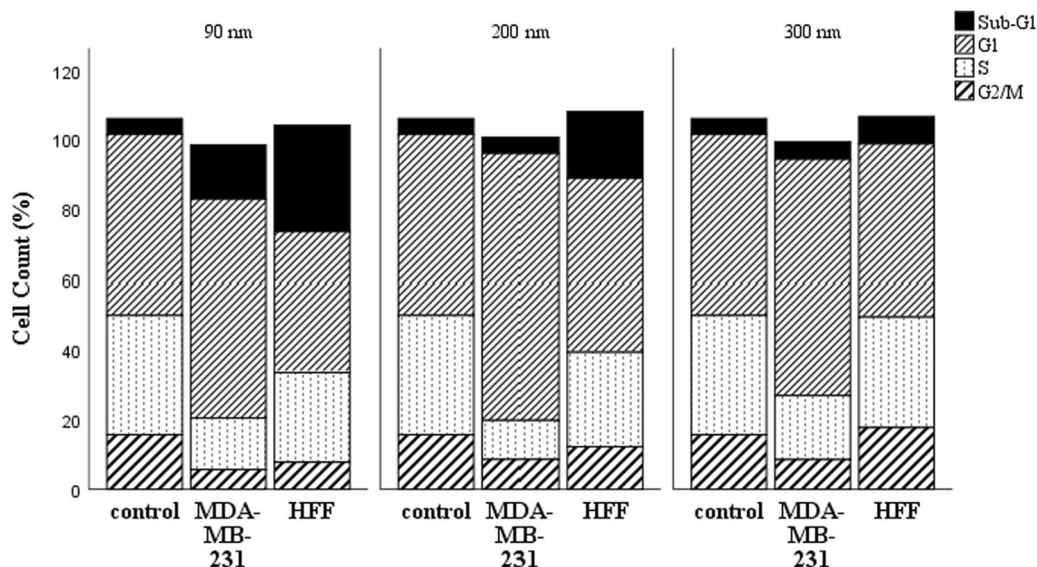


Fig. 10 Comparison of cell cycle phases in MDA-MB-231 and HFF-2 cells treated with PS-NH₂ with the control group after 48 h ($P < 0.001$)

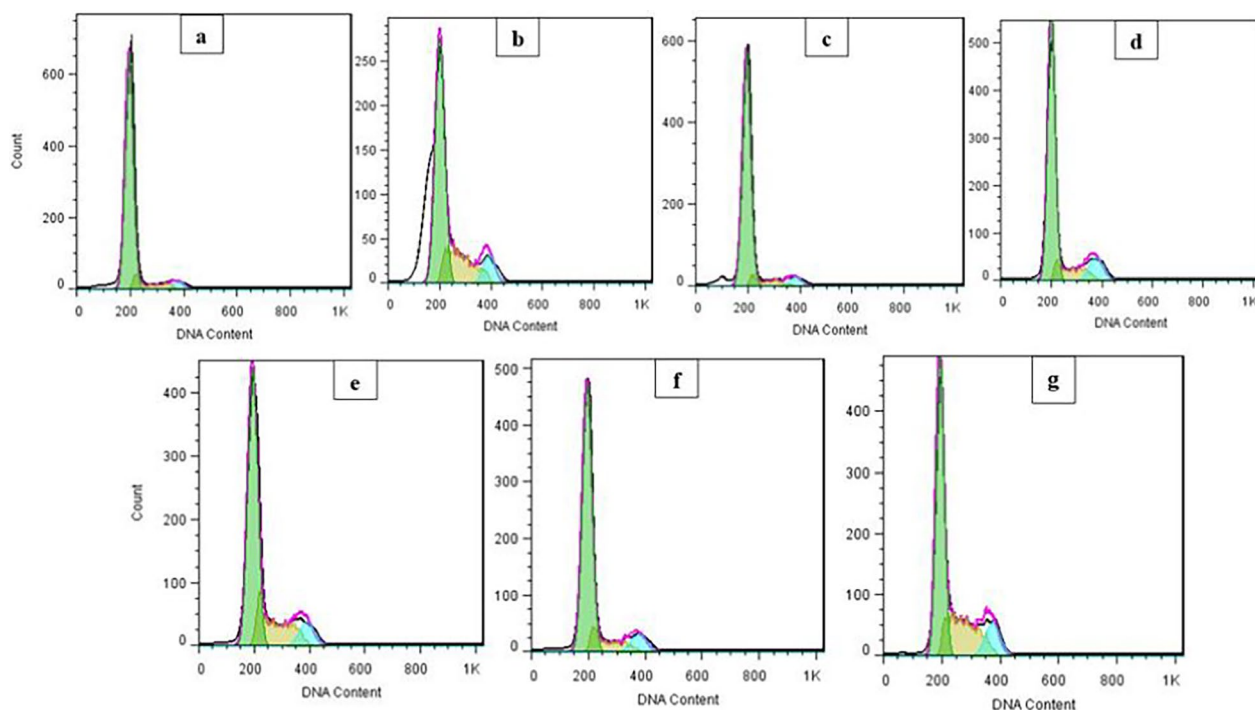


Fig. 11 Cell cycle results of MDA-MB 231 cells exposed to PS-NH₂ after 48 h. **a** 500 µg/ml size 90 nm. **b** 2000 µg/ml size 90 nm. **c** 500 µg/ml size 200 nm. **d** 2000 µg/ml size 200 nm. **e** 500 µg/ml size 300 nm. **f** 2000 µg/ml size 300 nm. **g** Cell as a control without the presence of C after 48 h

nanoparticles with a size of 200 nm at a concentration of 500 µg/ml, the enzyme activity increased by approximately 2.2 times compared to the control. At a concentration of 1000 µg/ml, the enzyme activity increased by 1.3 times compared to the control. Among the tested groups, as the concentration of PS-NH₂ increased,

enzyme activity decreased to about 0.68 times that of the control, and this difference was statistically significant ($P < 0.001$).

GPx enzyme activity was measured in HFF-2 cells compared to the control. According to the obtained results, after the cells were exposed to PS-NH₂ nanoparticles

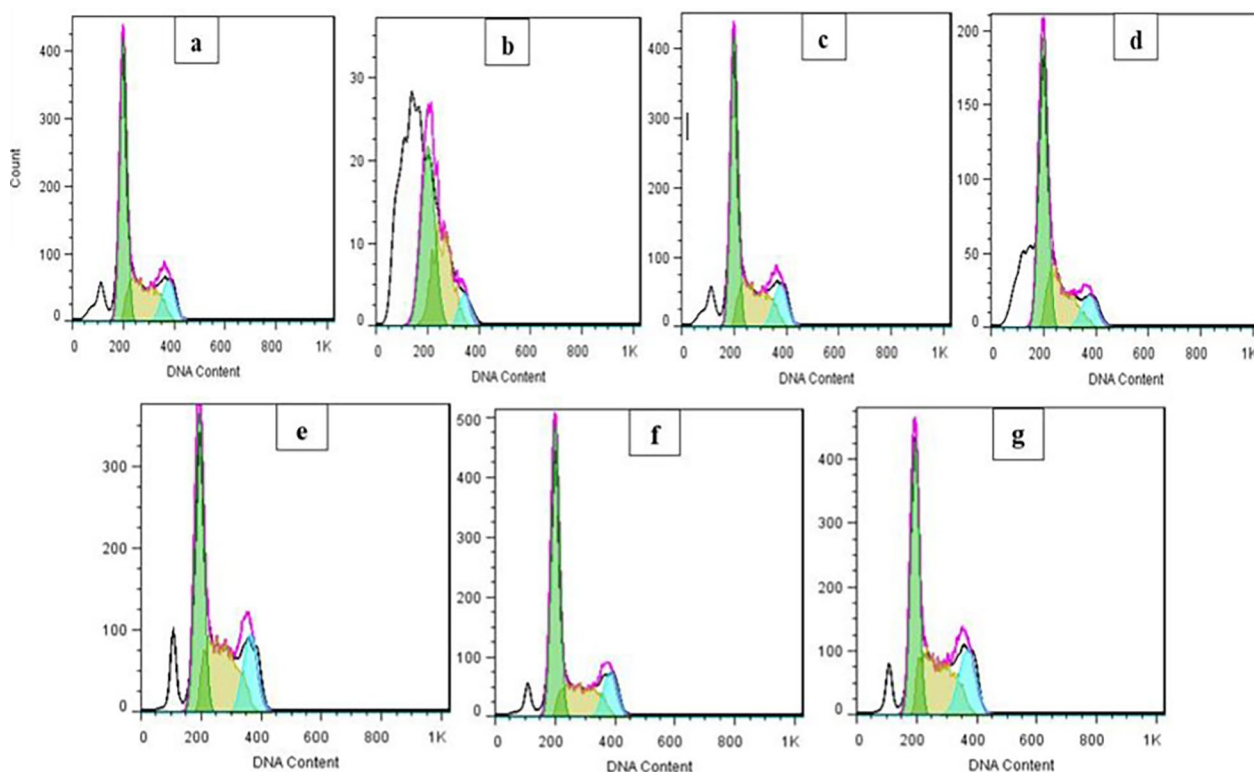


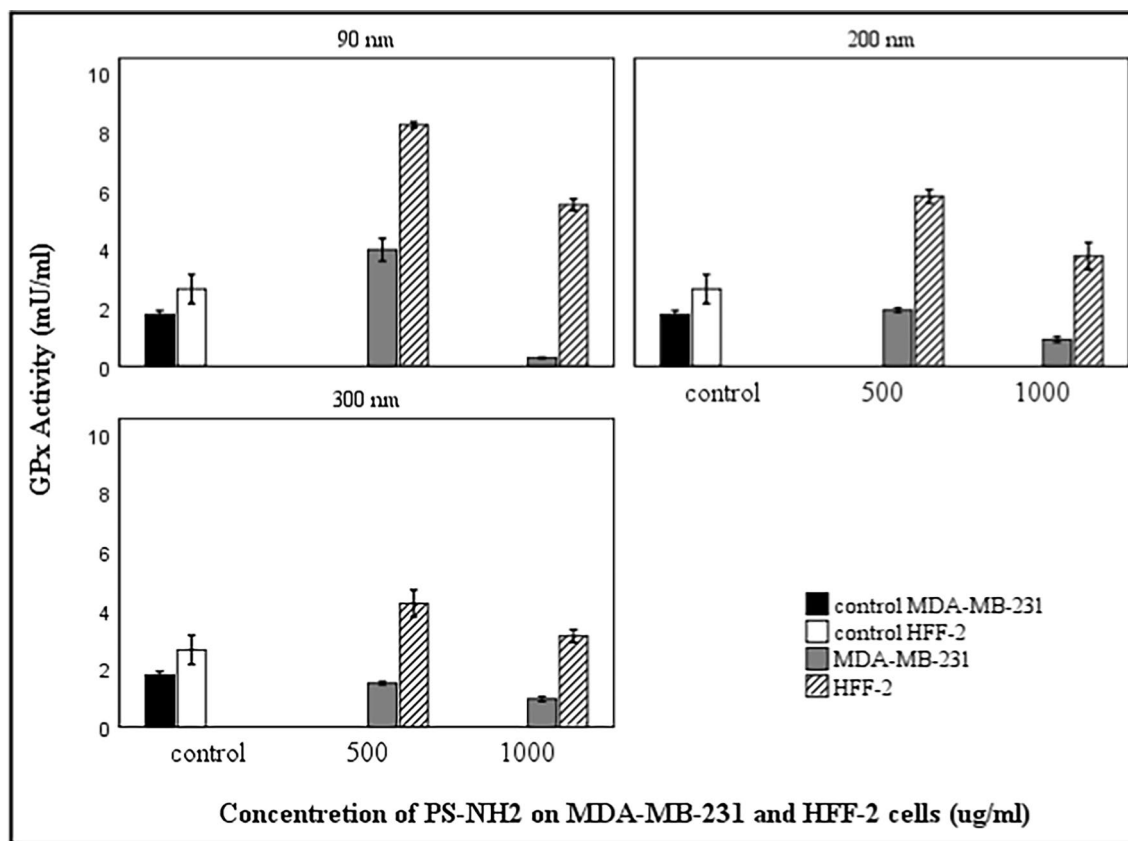
Fig. 12 Cell cycle results HFF-2 cells exposed to PS-NH₂ after 48 h. **a** 500 µg/ml size 90 nm. **b** 2000 µg/ml size 90 nm. **c** 500 µg/ml size 200 nm. **d** 2000 µg/ml size 200 nm. **e** 500 µg/ml size 300 nm. **f** 2000 µg/ml size 300 nm. **g** HFF-2 cells as a control without the presence of PS-NH₂ after 48 h

with a size of 300 nm at a concentration of 500 µg/ml, the enzyme activity increased by 1.5 times compared to the control. At a concentration of 1000 µg/ml, it increased by 1.2 times compared to the control. Among the tested groups, as the concentration of PS-NH₂ increased, enzyme activity decreased to about 0.68 times that of the control, and this difference was statistically significant ($P < 0.001$). Thus, the results of the present study indicate that with an increase in PS-NH₂ concentration, the level of GPx enzyme activity in HFF-2 cells decreases.

Glutathione is the most important intracellular non-protein antioxidant. This substance reduces free radicals in the cell; therefore, a reduction in the level of glutathione increases the amount of free radicals and induces apoptosis in cancer cells. The results of measuring GPx enzyme activity in our research indicated that the combination of PS-NH₂ in sizes of 90 nm, 200 nm, and 300 nm caused an increase in intracellular glutathione levels by 3, 2.2, and 1.2 times, respectively, compared to the control group in HFF-2 cells. In the MDA-MB-231 cell line, this nanoparticle at sizes of 90 nm and 200 nm increased intracellular glutathione levels by 2.2 and 1.1 times, respectively, compared to the control group, while at a size of 300 nm, enzyme activity was halved compared to the control (Fig. 13). In this cell line,

as the concentration of nanoparticles increased, there was a 13-fold decrease in GPx enzyme activity, which prevents the induction of apoptosis by increasing glutathione levels. In both cell lines, a statistically significant difference was observed compared to the control group ($p < 0.001$).

SOD is the cell's first line of defense against reactive oxygen species (ROS). Typically, the superoxide radical is the first free radical produced during stress, and SOD rapidly converts the superoxide radical into hydrogen peroxide and molecular oxygen. By removing superoxide, SOD plays a more vital role in the antioxidant system than catalase and peroxidase, thereby enhancing the resistance of cells to environmental stresses [29–31]. In most studies, the level of SOD activity is variable. This variability is partly due to differences in the tested factors, such as cell type, type of treatment, concentration of treatment, and duration of treatment [32]. The increase in SOD activity is attributed to its role in combating oxidative stress and protecting the cell's defense system against oxidative damage. Additionally, the rise in enzyme activity is likely due to an increase in superoxide levels, which may enhance the expression of superoxide dismutase genes through a signaling mechanism (Fig 13) [33]. By examining the activity of the superoxide



Error bars: +/- 2 SE

Fig. 13 Analysis of glutathione peroxidase enzyme (GPx mU/ml) on MDA-MB-231 and HFF-2 cells after treatment with 500, 1000 µg/ml of PS-NH₂ combination in three sizes 90, 200 and 300 nm

dismutase enzyme in MDA-MB-231 and HFF-2 cells treated for 48 hours with concentrations of 500 and 1000 µg/ml of the PS-NH₂ combination, it was observed that enzyme activity increased at lower treatment concentrations. However, enzyme activity decreased with increasing treatment concentration. The decrease in enzyme activity at high concentrations is likely due to the increased production of H₂O₂ within the cell, which can inactivate the enzyme, or it may result from the binding of PS-NH₂ to the active site of the enzyme, ultimately leading to reduced enzyme activity [34].

Statistical analysis of the data obtained from the measurement of superoxide dismutase enzyme activity using one-way ANOVA revealed that the enzyme activity in MDA-MB-231 and HFF-2 cells treated with PS-NH₂ was significantly different compared to the control ($P < 0.001$). Comparison of the average activity of the superoxide dismutase enzyme in HFF-2 cells showed that treatment with concentrations of 500 and 1000 µg/ml of PS-NH₂ increased the activity of this enzyme compared

to the control; however, with increasing concentration, the enzyme activity decreased. In MDA-MB-231 cells, compared to the control group, the activity of the SOD enzyme decreased, with higher concentrations of nanoparticles also leading to decreased enzyme activity. The highest activity of the superoxide dismutase enzyme was observed at a concentration of 500 µg/ml in HFF-2 cells, indicating an increase in SOD enzyme activity compared to the control group (Fig. 14).

In both normal and oxidative stress conditions, advanced antioxidant defense systems work to eliminate excess reactive oxygen species (ROS) in cells. For example, SOD is known to convert superoxide into H₂O₂ (Nordberg & Arner, 2001). Environmental pollutants can induce ROS production and subsequent oxidative stress. Overall, SOD is responsible for maintaining the dynamic balance between ROS production and scavenging under normal conditions. Therefore, SOD activity serves as an indicator of the antioxidant capacity of cells.

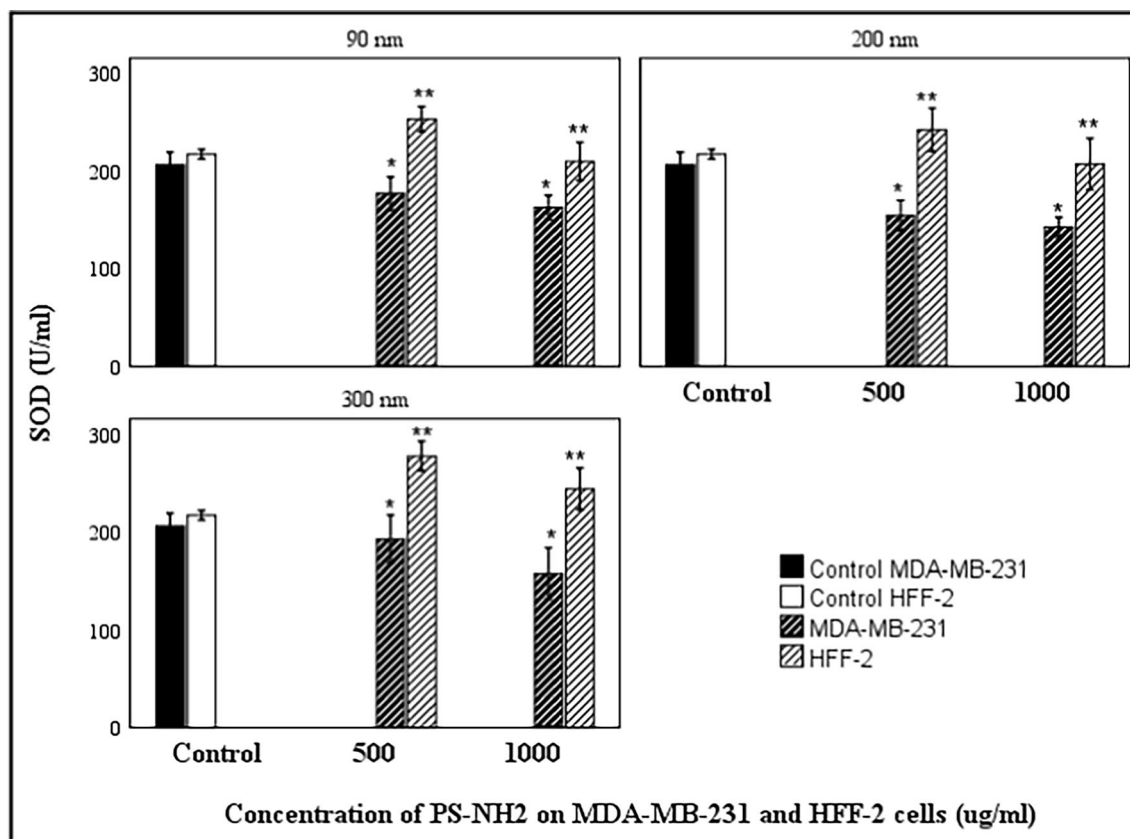


Fig. 14 Analysis of superoxide dismutase enzyme (SOD mU/ml) on MDA-MB-231 and HFF-2 cells after treatment with 500, 1000 µg/ml of PS-NH₂ combination in three sizes 90, 200 and 300 nm

Discussion

Polystyrene is one of the most common plastics used across various industries. It is made from styrene monomers and is utilized in the production of a wide range of products, including toys, cup covers, CDs, and items in the health and cosmetic industries, among others [3, 35]. According to recent studies, polystyrene nanoplastics have been detected in the human body. A Dutch study published in the journal *Environment International* recently discovered microplastics in human blood for the first time, raising concerns that these ubiquitous particles may also accumulate in organs.

The results of the infrared (IR) spectrum analysis related to polystyrene nanoplastics confirmed the presence of amino bonds in these nanoparticles. Images captured by a field emission scanning electron microscope (FESEM) showed that PS-NPs were synthesized in a spherical shape with a uniform and regular appearance.

In the zeta potential analysis of PS-NPs, it was found that a higher value (whether positive or negative) indicates greater stability in the colloidal dispersion. The examination revealed that PS-NH₂ nanoparticles exhibited a zeta potential close to zero, indicating that the

sample is nearly at its isoelectric point and possesses a neutral electric charge. Therefore, the obtained results suggest that PS-NH₂ nanoparticles, due to their surface charge range, may cause particle instability, leading to aggregation rather than separation (Fig. 1c) [17].

The results of the MTT assay indicate that the survival of MDA-MB-231 and HFF-2 cells is influenced by the concentration, size, and duration of exposure to polystyrene nanoplastics. In this research, it was observed that higher concentrations and smaller sizes of PS-NH₂ exhibited more cytotoxic effects compared to lower concentrations and larger sizes of this compound, as evidenced by morphological changes such as reduced cell volume and rounding. Additionally, PS-NH₂ nanoplastics significantly decreased cell viability with increasing concentration (Figs. 4, 5). The results of the MTT assay at concentrations of 10, 50, and 100 µg/ml clearly demonstrated that PS-NH₂, at the sizes used in this study, did not exhibit specific cytotoxic effects in vitro [20]. Furthermore, as the concentration of PS-NH₂ exceeded 125 µg/ml, cell viability decreased logarithmically [36].

The IC₅₀ values for the 90 nm, 200 nm, and 300 nm polystyrene nanoplastics were approximately 500 µg/

ml for 72 h and 250 µg/ml for 24 h. The results suggest that polystyrene nanoplastics possess cytotoxic potential against MDA-MB-231 and HFF-2 cell lines. The highest toxicity was observed for the 90 nm particles at a concentration of 2000 µg/ml over 72 h. Due to their smaller size, these nanoparticles have a greater ability to penetrate cells, resulting in significantly higher lethality and, consequently, a lower number of living cells in these wells.

Additionally, based on the research findings of Bamre et al. [27], it has been reported that no microbial decomposition is observed in polystyrene sheets buried in the soil after 32 years. Hydrophobic groups in thermoplastics have made them resistant to hydrolysis [37]. The molecular compounds in plastic affect the hydrophobicity of the polymer surface and facilitate the easy connection of microorganisms to one another on the plastic surface [38]. The high molecular weight and low solubility of polystyrene in water have prevented it from dissolving. These polymers pass through the membranes of microorganisms, and intracellular decomposition takes place on them. The biological process of decomposing these compounds begins with the release of extracellular enzymes from the decomposing microorganisms [38]. According to the results of studies by Lithner and his colleagues [39], most plastics are very resistant to microbial degradation in everyday use. The results of the MIC and dilution agar tests were also confirmatory and proved that PS-NH₂ nanoparticles have no antibacterial effect on bacteria, including *Staphylococcus aureus* and *E. coli* (Fig. 7), [27].

Apoptosis is defined as programmed cell death. If this process is disturbed, it can lead to pathological conditions, such as cancer and autoimmune disorders [40]. Unlike apoptosis, necrosis is the pathological death of cells, and this type of cell death occurs during severe damage to cells, such as hypoxia, hyperthermia, and exposure to external toxins. Radiotherapy, chemotherapy, and hormone therapy all induce apoptosis in cancer cells. However, using higher doses of these compounds can cause cancer cell death through other mechanisms [40].

PS-NH₂ in HFF-2 cells induced a peak of phosphatidylserine (one of the reliable indicators of apoptosis) in the flow cytometry histogram compared to the control group. Statistically, there is a significant difference compared to the control group ($P < 0.001$).

Increasing the concentration of PS-NH₂ (from 500 to 2000 nm) leads to an increase in the percentage of necrosis and apoptosis in both MDA-MB-231 and HFF-2 cell lines. In the MDA-MB-231 cell line, the necrosis percentage increases from 7.6% to 20%, and the late apoptosis percentage rises from 16.6% to 35.7%. Similarly, in the HFF-2 cell line, the necrosis percentage increases from 8.97% to 15.4%, while late apoptosis decreases from

42.6% to 36.1%, indicating a greater sensitivity of HFF-2 cells to nanoplastics at lower concentrations.

In both cell lines, increasing the nanoplastic concentration results in a rise in cell death (necrosis and apoptosis). However, early apoptosis is observed at a lower percentage at higher concentrations, which may suggest a progression toward late apoptosis. The percentage of viable cells decreases as the concentration of nanoplastics increases. For MDA-MB-231 cells, viability decreases from 74% at 500 nm to 43.4% at 2000 nm, whereas in HFF-2 cells, it ranges from 40.2% to 42% across different concentrations.

The effects of polystyrene on these two cell types may proceed via the following pathways:

Activation of apoptotic signaling pathways: polystyrene may activate specific proteins that induce apoptosis, potentially involving caspase activation and the upregulation of genes associated with cell death.

Mitochondrial dysfunction: this dysfunction can lead to increased free radical production, ultimately resulting in necrosis and cell death. Polystyrene may induce necrosis, often due to severe damage to cell membranes and disruption of metabolic processes.

Overall, polystyrene has distinctly different impacts on MDA-MB-231 and HFF-2 cell types. While MDA-MB-231 cells exhibit greater resistance to increasing polystyrene particle size, HFF-2 cells are more susceptible to necrosis and apoptosis.

The general conclusion that can be drawn is that smaller-sized polystyrene nanoplastics at higher concentrations exhibit greater toxicity over time. This research observed that the toxic effect of PS-NH₂ on fibroblast cells is greater than on cancer cells, which serves as a warning regarding the extensive use of products containing these nanoparticles (Figs. 8,9a–g). These findings are valuable for toxicology studies and for the design of nanomaterials in biomedical and materials science fields.

The results of the cell cycle analysis showed that MDA-MB-231 cells treated with amine-modified polystyrene at all concentrations exhibited significant arrest in the G1 phase over time compared to the control cells. Increasing the concentration of treatment caused a slight decrease in the percentage of cells in the S and G2 phases. In HFF-2 cells, increasing the concentration of treatment led to a slight increase in the percentage of cells in the G1, S, and G2 phases.

In HFF-2 cells, a significant increase was observed in the sub-G1 population, which indicates the occurrence of apoptosis. In MDA-MB-231 cells, this increase occurred only at the nanoparticle size of 90 nm.

The mean results and standard deviations showed statistically significant differences compared to the control ($P < 0.001$). Additionally, the percentage of cells entering

the sub-G1 phase, indicating apoptotic cells, increased significantly depending on the dose and size of the nanoparticles in both cell lines compared to the control (Fig. 10).

Based on these results, it can be concluded that the inhibitory effects of PS-NH₂ on MDA-MB-231 and HFF-2 cell lines likely occur through the activation of the apoptotic pathway (Figs. 10 and 11).

In a study by Hu et al. [41] investigating the effects of PS-NPs on zebrafish larvae and macrophage cells, the results showed that the percentage of apoptotic cells in the early stages was higher in the PS-NPs group compared to the control group. The percentage of apoptotic cells increased in a concentration-dependent manner, with a maximum increase of about 10%. They also identified caspase-3 protease activity in zebrafish larvae, which plays a central role in the execution of apoptosis. Their findings demonstrated that PS-NPs treatment induced a certain degree of apoptosis.

In a study on the effect of microplastic polystyrene (PS-MPs) on granulosa cells (GCs) in rat ovaries, An et al. [42] observed that treatment with this compound induces apoptosis. Their study showed that the apoptosis rate of granulosa cells significantly increased after treatment with PS-MPs. These results indicate that PS-MPs induce apoptosis in GCs through oxidative stress.

The glutathione system plays a vital role in protecting the body from oxidative stress. This system converts hydrogen peroxide produced by the activity of the superoxide dismutase enzyme on superoxide ions, a dangerous reactive oxygen species (ROS), into water. Glutathione peroxidase and glutathione reductase are enzymes essential to this cycle, and the expression of their genes increases when ROS levels rise, placing the body in a state of oxidative stress. The reason for the specific examination of antioxidant enzymes, particularly glutathione peroxidase (GPx), is that these enzymes play a vital role in protecting cells against oxidative stress. In conditions where PS-NH₂ induce the production of reactive oxygen species (ROS), measuring the activity of these enzymes can serve as an indicator of the cells' ability to cope with oxidative damage.

Moreover, an increase in the levels of antioxidant enzymes reflects the cells' response to oxidative stress and can illuminate the impact of nanoplastics on cell health and the extent of cell death (apoptosis and necrosis). Investigating these enzymes can enhance our understanding of the mechanisms of nanoplastic toxicity and potential ways to protect cells from damage caused by them. Oxidative stress induced by reactive oxygen species causes apoptosis and destruction in both cancerous and non-cancerous cells. Research on these particles indicates a notable relationship between particle size and the

capacity to produce reactive oxygen species (ROS), which is influenced by their physicochemical characteristics. In particular, smaller particles are taken up more efficiently, resulting in higher levels of ROS generation [43–46].

The effects of ROS can manifest at physiological, cellular, and genetic levels, potentially progressing to stages of tumorigenesis [47].

GSH acts as a strong scavenger of free radicals and is also responsible for maintaining the cellular redox state, protecting cells against oxidative stress [48]. The content of GSH in HFF-2 cells exposed to PS-NH₂ significantly increased compared to the control group ($P < 0.001$), indicating a strong induction of oxidative stress. Exposure to 500 µg/ml of PS-NH₂ at a size of 90 nm resulted in the maximum increase in GSH content. In HFF-2 cells treated with PS-NH₂ nanoparticles, we observed less GPx activity with increasing particle size; at 90 nm, the activity of the GPx enzyme increased by about three times compared to the control. At 200 and 300 nm sizes, the level of GPx enzyme activity increased by two and one times, respectively, compared to the control.

In MDA-MB-231 cells, which are cancerous and have experienced more damage, the level of GPx enzyme activity was lower than that of the control group. Additionally, with the increase in the size of the nanoparticles, we observed a decrease in enzyme activity. The level of GPx enzyme in MDA-MB-231 cells is lower than that in HFF-2 cells, showing a statistically significant difference compared to the control group (Fig. 13) ($P < 0.001$).

The increase in SOD activity and GSH content in HFF-2 and MDA-MB-231 cells at higher doses of PS-NH₂ indicates impairment of antioxidant capacities, which play a fundamental role in eliminating superoxide anions (O₂⁻) and H₂O₂. An imbalanced antioxidant capacity against oxidative stress causes disturbances in antioxidant structures, ultimately leading to cell death. In the electron transfer chain, O₂⁻ is produced by the reduction of oxygen molecules, accompanied by the leakage of electrons. After its production, O₂⁻ can be spontaneously converted to H₂O₂ by SOD. Additionally, H₂O₂ can be reduced by enzymatic antioxidants such as glutathione peroxidase (GPx), where GSH acts as an exclusive electron donor [49]. This is consistent with previous studies indicating that the cytotoxicity of nanoparticles is dependent on surface charge [50] and concentration [51].

PS-NH₂ significantly decreased SOD activity and prevented the increase in GSH content. Previous studies have reported that the inhibition of SOD activity leads to the accumulation of O₂⁻ [52] and GSH is necessary to reduce H₂O₂-induced oxidative damage [53].

During a study of the effect of PS-NH₂ nanoparticles on HepG2 cells, He et al. [20] showed that SOD enzyme activity decreases with increasing concentration

after treatment with these particles. Our results in this research are consistent with their findings, as we observed a decrease in enzyme activity with increasing treatment concentration in both MDA-MB-231 and HFF-2 cells.

An et al. [42] showed the effect of polystyrene microplastics (PS-MPs) on granulosa cells (GCs) in rat ovaries, finding that PS-MPs lead to an increase in MDA enzyme levels and a decrease in GSH-PX, CAT, and SOD in ovarian tissue. Furthermore, the level of ROS was significantly higher in GCs treated with PS-MPs. Our results indicated that PS-NH₂ nanoparticles decrease SOD and GPx enzyme levels compared to the control group, aligning with the findings of An et al., who reported that PS-MPs cause oxidative stress in the ovaries of rats.

Conclusion

MDA-MB-231 cells: The toxicity of PS-NH₂ nanoparticles increases with higher concentrations and longer exposure. As the concentration increases, the percentage of living cells decreases, leading to significant apoptosis. **HFF-2 cells:** Similar trends in toxicity are observed, but there is a notable difference in the response. The cell death results indicate that polystyrene at smaller sizes (90 nm) increases necrosis and late apoptosis in HFF-2 cells, suggesting a higher sensitivity of these cells to PS-NH₂ toxicity. This cell death is most likely due to membrane damage and elevated oxidative stress. In contrast, MDA-MB-231 cells demonstrate greater resistance, maintaining a higher percentage of viable cells as the polystyrene size increases. This difference may result from the enhanced tolerance of MDA-MB-231 cells to stress and their reparative mechanisms. These variations are likely attributable to the distinct cellular composition, structure, and signaling pathways in these two cell types. Smaller nanoparticle sizes correlate with greater toxicity effects. Conversely, as the size of the nanoparticles increases, the cytotoxic effects decrease in both MDA-MB-231 and HFF-2 cells. MDA-MB-231 Cells primarily arrest in the G1 and sub-G1 phases, which is indicative of apoptosis due to treatment with PS-NH₂ nanoparticles. HFF-2 cells also show arrest in the G1 and sub-G1 phases, but demonstrate higher levels of apoptosis compared to MDA-MB-231 cells. MDA-MB-231 cells' apoptosis is the main form of cell death induced by PS-NH₂ nanoparticles, indicating a more programmed cell death response. In HFF-2 cells, higher incidences of necrosis are observed, suggesting that normal cells may not respond to stress in the same manner as cancer cells, which may indicate a different underlying mechanism of toxicity.

Glutathione peroxidase (GPx) activity in both cell types indicates that an increase in nanoparticle concentration

correlates with a decrease in GPx activity, leading to higher free radical levels, which in turn promote apoptosis in cancer cells. HFF-2 cells maintain higher levels of glutathione, which may help prevent apoptosis. Superoxide dismutase (SOD) activity treatment with PS-NH₂ nanoparticles leads to increased SOD activity initially. However, at higher concentrations, SOD activity decreases, indicating a potential impairment in the antioxidant defense mechanism in both cell types. The imbalance in antioxidant capacity can contribute to oxidative stress and cell death.

The results indicate that PS-NH₂ nanoparticles have contradictory effects on MDA-MB-231 cells and HFF-2 cells. These effects can be explained by changes in the activity of antioxidant enzymes and GSH levels, as well as the induction of oxidative stress and cellular damage. Therefore, PS-NH₂ may act as a potential agent for inducing oxidative damage in MDA-MB-231 cells while simultaneously stimulating defensive mechanisms in HFF-2 cells. **MDA-MB-231 vs. HFF-2:** While both cell types exhibit toxicity from PS-NH₂ nanoparticles, MDA-MB-231 cells are more prone to apoptosis, whereas HFF-2 cells show a greater tendency toward necrosis. This difference underscores the distinct responses of cancerous and normal cells to nanoparticle treatment, which could have implications for therapeutic strategies using such materials. This analysis highlights the complex interactions between PS-NH₂ nanoparticles and cellular responses in cancer versus normal cells, revealing important distinctions that may guide future research and applications in cancer therapy.

Abbreviations

ANOVA	Analysis of variance
CAT	Catalase
<i>E. coli</i>	<i>Escherichia coli</i>
GPx	Glutathione peroxidase
HFF-2	Human fetal fibroblasts
IC50	The half-maximal inhibitory concentration
MDA	Malondialdehyde
MDA-MB-231	Breast cancer cell line
PS-MPs	Polystyrene microplastics
PS-NH ₂	Polystyrene-amine
PS-NPs	Polystyrene nanoplastics
ROS	Reactive oxygen species
<i>S. aureus</i>	<i>Staphylococcus aureus</i>
SOD	Superoxide dismutase

Acknowledgements

The authors would like to thank the Women's Research Institute of Al-Zahra University.

Author contributions

H.S. was the first author and designed and performed all the experiments. P. H. was the supervisor and provided the financial resources. H.S. and R.R. jointly analyzed the results of the experiments. S.K. was the consultant. H.S. wrote this version and added new ideas to the work. R.R. and S.K. read the final version of the manuscript and approved it for submission. H.S. is the first author and P.H. is the corresponding author.

Funding

Prichher Hanachi provided financial resources.

Availability of data and materials

No datasets were generated or analysed during the current study.

Declarations**Ethics approval and consent to participate**

This declaration is "not applicable".

Competing interests

The authors declare no competing interests.

Author details

¹Department of Biotechnology, Faculty of Biological Sciences, Alzahra University, Tehran, Iran. ²Department of Family Therapy, Women Research Center, Alzahra University, Tehran, Iran.

Received: 17 September 2024 Accepted: 10 November 2024

Published online: 02 January 2025

References

- Kik K, Bukowska B, Sicińska P (2020) Polystyrene nanoparticles: sources, occurrence in the environment, distribution in tissues, accumulation and toxicity to various organisms. *Environ Pollut*. <https://doi.org/10.1016/j.envpol.2020.114297>
- Tomita K et al (2019) Lipid peroxidation increases hydrogen peroxide permeability leading to cell death in cancer cell lines that lack mtDNA. *Cancer Sci* 110(9):2856–2866. <https://doi.org/10.1111/cas.14132>
- Kik K, Sici P (2020) Polystyrene nanoparticles: Sources, occurrence in the environment, distribution in tissues, accumulation and toxicity to various organisms. *Environ Poll.* 1;262:114297. <https://doi.org/10.1016/j.envpol.2020.114297>
- Waring R (2018) Plastic contamination of the food chain. A threat to human health. *Maturitas*. 1;115:64–8 <https://doi.org/10.1016/j.maturitas.2018.06.010>
- Blettler MCM, Abrial E, Khan FR, Sivri N, Espinola LA (2018) Freshwater plastic pollution: recognizing research biases and identifying knowledge gaps. *Water Res* 143:416–424. <https://doi.org/10.1016/j.watres.2018.06.015>
- Rafiee M et al (2018) Neurobehavioral assessment of rats exposed to pristine polystyrene nanoplastics upon oral exposure. *Chemosphere* 193:745–753. <https://doi.org/10.1016/j.chemosphere.2017.11.076>
- Wen B, Zhang N, Jin S, Chen Z, Gao J (2018) Microplastics have a more profound impact than elevated temperatures on the predatory performance, digestion and energy metabolism of an Amazonian cichlid. *Aquat Toxicol* 195:67–76. <https://doi.org/10.1016/j.aquatox.2017.12.010>
- Zhang W, Liu Z, Tang S, Li D, Jiang Q, Zhang T (2020) Transcriptional response provides insights into the effect of chronic polystyrene nanoplastic exposure on *Daphnia pulex*. *Chemosphere* 238:124563. <https://doi.org/10.1016/j.chemosphere.2019.124563>
- Sung H et al (2021) Global cancer statistics 2020: GLOBOCAN estimates of incidence and mortality worldwide for 36 cancers in 185 countries. *CA Cancer J Clin* 71(3):209–249. <https://doi.org/10.3322/caac.21660>
- Schirinzi GF, Pérez-Pomeda I, Sanchís J, Rossini C, Farré M, Barceló D (2017) Cytotoxic effects of commonly used nanomaterials and microplastics on cerebral and epithelial human cells. *Environ Res* 159:579–587
- Anguissola S, Garry D, Salvati A, O'Brien PJ, Dawson KA (2014) High content analysis provides mechanistic insights on the pathways of toxicity induced by amine-modified polystyrene nanoparticles. *PLoS ONE*. <https://doi.org/10.1371/journal.pone.0108025>
- Forte M et al (2016) Polystyrene nanoparticles internalization in human gastric adenocarcinoma cells. *Toxicol. Vitr.* 31:126–136. <https://doi.org/10.1016/j.tiv.2015.11.006>
- Pan I, Umapathy S, Issac PK et al (2023) The bioaccessibility of adsorbed heavy metals on biofilm-coated microplastics and their implication for the progression of neurodegenerative diseases. *Environ Monit Assess* 195:1264. <https://doi.org/10.1007/s10661-023-11890-7>
- Kandaswamy K, et al (2024) Polystyrene nanoplastics synergistically exacerbate diclofenac toxicity in embryonic development and the health of adult zebrafish. *Comp Biochem Physiol Part C Toxicol Pharmacol* 281:109926
- Boopathi S et al (2023) Combined effects of a high-fat diet and polyethylene microplastic exposure induce impaired lipid metabolism and locomotor behavior in larvae and adult zebrafish. *Sci Total Environ* 902:165988. <https://doi.org/10.1016/j.scitotenv.2023.165988>
- Guru A, Rady A, Darwish NM, Malafaia G, Arokiyaraj S, Arockiaraj J (2023) Synergistic effects of polyethylene microplastic and abamectin pesticides on the eyes of zebrafish larvae and adults through activation of apoptosis signaling pathways. *Environ Toxicol Pharmacol* 102:104215
- Fadare OO, Wan B, Guo LH, Xin Y, Qin W, Yang Y (2019) Humic acid alleviates the toxicity of polystyrene nanoplastic particles to: *Daphnia magna*. *Environ Sci Nano* 6(5):1466–1477. <https://doi.org/10.1039/c8en01457d>
- Xu M et al (2019) Internalization and toxicity: a preliminary study of effects of nanoplastic particles on human lung epithelial cell. *Sci Total Environ* 694:133794
- Gerlier D, Thomasset N (1986) Use of MTT colorimetric assay to measure cell activation. *J Immunol Methods* 94(1–2):57–63. [https://doi.org/10.1016/0022-1759\(86\)90215-2](https://doi.org/10.1016/0022-1759(86)90215-2)
- He Y et al (2020) Cytotoxic effects of polystyrene nanoplastics with different surface functionalization on human HepG2 cells. *Sci Total Environ* 723:138180. <https://doi.org/10.1016/j.scitotenv.2020.138180>
- Nagavi-alhoseiny AA, Torshabi M, Rasoulianboroujeni M, Tayebi L, Tabatabaei FS (2019) Effect of sodium chloride on gene expression of *Streptococcus mutans* and zeta potential of demineralized dentin. *J Oral Biol Craniofac Res* 9(1):1–4. <https://doi.org/10.1016/j.jobocr.2018.08.002>
- Ruiz-Palacios M, Almeida M, Martins MA, Oliveira M, Esteban MÁ, Cuesta A (2020) Establishment of a brain cell line (FuB-1) from mummichog (*Fundulus heteroclitus*) and its application to fish virology, immunity and nanoplastics toxicology. *Sci Total Environ* 708:134821
- Cortés C, Domenech J, Salazar M, Pastor S, Marcos R, Hernández A (2020) Nanoplastics as a potential environmental health factor: effects of polystyrene nanoparticles on human intestinal epithelial Caco-2 cells. *Environ Sci Nano* 7(1):272–285
- Liu Y et al (2011) Intracellular dynamics of cationic and anionic polystyrene nanoparticles without direct interaction with mitotic spindle and chromosomes. *Biomaterials* 32(32):8291–8303
- Kawata K, Osawa M, Okabe S (2009) In vitro toxicity of silver nanoparticles at noncytotoxic doses to HepG2 human hepatoma cells. *Environ Sci Technol* 43(15):6046–6051
- Xia T, Kovochich M, Liong M, Zink JI, Nel AE (2008) Cationic polystyrene nanosphere toxicity depends on cell-specific endocytic and mitochondrial injury pathways. *ACS Nano* 2(1):85–96. <https://doi.org/10.1021/nn700256c>
- Bamre T, Naji A (2020) Toxicity of polystyrene nanoplastic (+ PS-NH₂) on *Chlorella vulgaris* microalgae. *Hormoz-jae* 10(2):52–62
- Futreal PA, Wooster R, Stratton MR (2005) Somatic mutations in human cancer: insights from resequencing the protein kinase gene family. *Cold Spring Harb Symp Quant Biol* 70:43–49. <https://doi.org/10.1101/sqb.2005.70.015>
- Gill SS, Tuteja N (2010) Reactive oxygen species and antioxidant machinery in abiotic stress tolerance in crop plants. *Plant Physiol Biochem* 48(12):909–930
- Bernardi R, Nali C, Gargiulo R, Pugliesi C, Lorenzini G, Durante M (2001) Protein pattern and Fe-superoxide dismutase activity of bean plants under sulphur dioxide stress. *J Phytopathol* 149(7–8):477–480
- Shi Q, Ding F, Wang X, Wei M (2007) Exogenous nitric oxide protect cucumber roots against oxidative stress induced by salt stress. *Plant Physiol Biochem* 45(8):542–550
- Chin L (2007) Investigations into lead (Pb) accumulation in *Symphytum officinale* L.: a phytoremediation study
- Kaur G, Singh HP, Batish DR, Kumar RK (2012) Growth, photosynthetic activity and oxidative stress in wheat (*Triticum aestivum*) after exposure of lead to soil. *J Environ Biol* 33(2):265
- Fatima RA, Ahmad M (2005) Certain antioxidant enzymes of *Allium cepa* as biomarkers for the detection of toxic heavy metals in wastewater. *Sci Total Environ* 346(1–3):256–273

35. Lithner D, Larsson A, Dave G (2011) Environmental and health hazard ranking and assessment of plastic polymers based on chemical composition. *Sci Total Environ* 2011 Aug 15;409(18):3309–24. <https://doi.org/10.1016/j.scitotenv.2011.04.038>
36. Chan PC, Xia Q, Fu PP (2007) *Ginkgo biloba* leave extract: biological, medicinal, and toxicological effects. *J Environ Sci Health Part C Environ Carcinog Ecotoxicol Rev* 25(3):211–244. <https://doi.org/10.1080/10590500701569414>
37. Hanachi P, Maleki M, Karbalae S (2020) Effect of polystyrene microplastic and chlorpyrifos pesticide on superoxide dismutase activity in tissues of rainbow trout (*Oncorhynchus mykiss*). *J Fish* 72(4):328–343
38. Ho BT, Timothy R, Steven L (2018) An overview on biodegradation of polystyrene and modified polystyrene: the microbial approach. *Crit Rev Biotechnol* 38(2):308–320
39. Lithner D, Larsson Å, Dave G (2011) Environmental and health hazard ranking and assessment of plastic polymers based on chemical composition. *Sci Total Environ* 409(18):3309–3324
40. Wyllie AH (1992) Apoptosis and the regulation of cell numbers in normal and neoplastic tissues an overview. *Cancer Metast Rev*. 1992 Sep;11:95–103. <https://doi.org/10.1007/BF00048057>
41. Hu Q, Wang H, He C, Jin Y, Fu Z (2021) Polystyrene nanoparticles trigger the activation of p38 MAPK and apoptosis via inducing oxidative stress in zebrafish and macrophage cells. *Environ Poll*. <https://doi.org/10.1016/j.envpol.2020.116075>
42. An R et al (2021) Polystyrene microplastics cause granulosa cells apoptosis and fibrosis in ovary through oxidative stress in rats. *Toxicology*. <https://doi.org/10.1016/j.tox.2020.152665>
43. Wick AF, Daniels WL, Orndorff ZW, Alley MM (2013) Organic matter accumulation post-mineral sands mining. *Soil Use Manag* 29(3):354–364. <https://doi.org/10.1111/sum.12058>
44. Yu F, Yang C, Zhu Z, Bai X, Ma J (2019) Adsorption behavior of organic pollutants and metals on micro/nanoplastics in the aquatic environment. *Sci Total Environ* 694:133643
45. Lei L, Liu M, Song Y, Lu S, Hu J, Cao C (2018) Polystyrene (nano) microplastics cause size-dependent neurotoxicity, oxidative damage and other adverse effects in *Caenorhabditis elegans*. *Environ Sci Nano* 5(8):2009–2020
46. Jeong C, Kang H, Lee M, Kim D, Han J (2017) Adverse effects of microplastics and oxidative stress-induced MAPK/Nrf2 pathway-mediated defense mechanisms in the marine copepod *Paracyclopina nana*. *Sci Rep* 7(1):1–11
47. Birben E, Sahiner M, Sackesen C, Erzurum S, Kalayci O (2012) Oxidative stress and antioxidant defense. *World Allergy Organ J* 5(1):9–19
48. Sharma A, Gorey B, Casey A (2019) In vitro comparative cytotoxicity study of aminated polystyrene, zinc oxide and silver nanoparticles on a cervical cancer cell line. *Drug Chem Toxicol* 42(1):9–23. <https://doi.org/10.1080/01480545.2018.1424181>
49. Luo J, Mills K, le Cessie S, Noordam R, van Heemst D (2019) Ageing, age related diseases and oxidative stress. What to do next. *Age Res Rev*. <https://doi.org/10.1016/j.arr.2019.100982>
50. Dausend J et al (2008) Uptake mechanism of oppositely charged fluorescent nanoparticles in HeLa cells. *Macromol Biosci* 8(12):1135–1143. <https://doi.org/10.1002/mabi.200800123>
51. Ware MJ et al (2014) Analysis of the influence of cell heterogeneity on nanoparticle dose response. *ACS Nano* 8(7):6693–6700. <https://doi.org/10.1021/nn502356f>
52. Ibrahim HR, Hoq MI, Aoki T (2007) Ovotransferrin possesses SOD-like superoxide anion scavenging activity that is promoted by copper and manganese binding. *Int J Biol Macromol* 41(5):631–640. <https://doi.org/10.1016/j.ijbiomac.2007.08.005>
53. Ren H, Meng Q, Yepuri N, Du X, Sarpong JO, Cooney RN (2018) Protective effects of glutathione on oxidative injury induced by hydrogen peroxide in intestinal epithelial cells. *J Surg Res* 222:39–47. <https://doi.org/10.1016/j.jss.2017.09.041>

Publisher's Note

Springer Nature remains neutral with regard to jurisdictional claims in published maps and institutional affiliations.